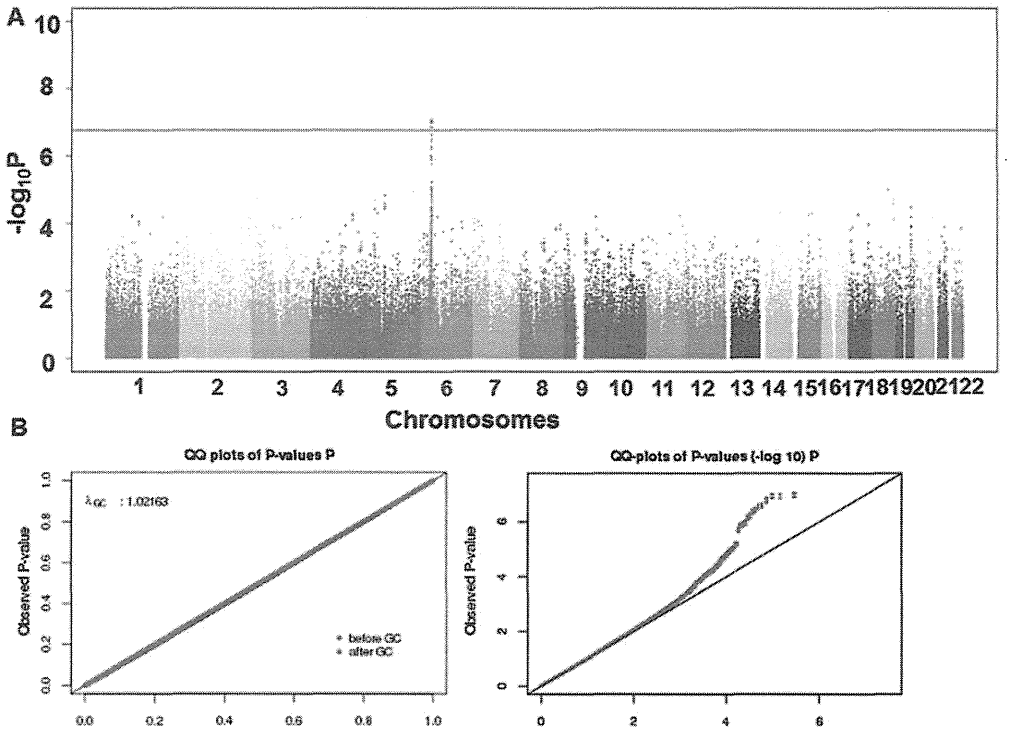

Figure 1. Genome-wide association study (GWAS) results for antinuclear antibody (ANA) production. **A,** Manhattan plot. The horizontal line indicates the significance level of the GWAS based on Bonferroni correction. **B,** Q–Q plots. λ_{gc} = genomic control inflation factor.

association of rs2395185 was replicated (overall $P = 1.3 \times 10^{-11}$) (Table 2).

SNP rs2395185 is located between the *HLA–DRA* and *HLA–DRB5* genes and is in moderate LD with HLA–DRB1*0405 ($r^2 = 0.42$). Considering that major histocompatibility complex proteins are respon-

Table 2. Associations of top SNPs with ANAs or their staining patterns*

SNP	Chr.	Position	ANA staining pattern	Nearest gene	Ref/var	Study	β	SE	OR (95% CI)	P
rs2395185	6	32541145	ANA (total)	*HLA–DRA*	G/T	GWAS	0.29	0.055	1.33 (1.20–1.48)	1.4×10^{-7}
						Replication	0.22	0.050	1.24 (1.12–1.37)	1.3×10^{-5}
						Overall	0.25	0.037	1.28 (1.19–1.38)	1.3×10^{-11}
rs2395185	6	32541145	Speckled	*HLA–DRA*	G/T	GWAS	0.29	0.055	1.33 (1.20–1.48)	1.4×10^{-7}
						Replication	0.22	0.050	1.25 (1.13–1.37)	8.3×10^{-6}
						Overall	0.25	0.037	1.29 (1.20–1.38)	7.5×10^{-12}
rs2395185	6	32541145	Homogeneous	*HLA–DRA*	G/T	GWAS	0.31	0.058	1.37 (1.22–1.54)	7.0×10^{-8}
						Replication	0.24	0.058	1.27 (1.13–1.42)	4.6×10^{-5}
						Overall	0.28	0.041	1.32 (1.22–1.43)	2.2×10^{-11}
rs6457300	6	31106721	Nucleolar	*C6orf205*	T/G	GWAS	−0.53	0.12	0.59 (0.46–0.74)	1.2×10^{-5}
						Replication	−0.13	0.11	0.88 (0.70–1.10)	0.26
						Overall	−0.32	0.083	0.73 (0.62–0.86)	0.00013
rs1611185	6	29876323	Discrete speckled	*HLA–G*	T/C	GWAS	1.28	0.29	3.61 (2.03–6.41)	1.2×10^{-5}
						Replication	0.19	0.25	1.21 (0.74–1.99)	0.44
						Overall	0.66	0.19	1.93 (1.32–2.80)	0.00060

* SNP = single-nucleotide polymorphism; ANAs = antinuclear antibodies; Chr. = chromosome; Ref/var = reference allele/variant allele; OR = odds ratio; 95% CI = 95% confidence interval; GWAS = genome-wide association study.

Table 3. Associations of SLE-related SNPs with ANA positivity and SLE susceptibility*

SNP	Chr.	Position	Gene	Ref/var	*P*	ANA OR (95% CI)†	SLE OR (95% CI)‡
Previous loci in Japanese population							
rs10168266	2	191644049	*STAT4*	T/C	0.20	1.08 (0.96–1.2)	1.59 (1.42–1.78)
rs340630	4	88177419	*AFF1*	A/G	0.13	1.08 (0.98–1.2)	1.21 (1.14–1.30)
rs9501626	6	32508322	*HLA*	A/C	0.62	1.04 (0.89–1.22)	1.86 (1.62–2.13)
rs2230926	6	138237759	*TNFAIP3*	G/T	0.15	1.16 (0.95–1.41)	1.75 (1.47–2.08)
rs6964720	7	75018280	*HIP1*	G/A	0.69	0.98 (0.86–1.1)	1.43 (1.27–1.63)
rs2254546	8	11381089	*BLK*	G/A	0.90	1.01 (0.9–1.13)	1.42 (1.25–1.61)
rs6590330	11	127816269	*ETS1*	A/G	0.015	1.14 (1.03–1.27)	1.44 (1.30–1.60)
Independent susceptibility SNPs of HLA locus in European population							
rs9265604	6	31407429	*HLA–B*	C/T	0.78	1.02 (0.92–1.13)	0.83 (0.78–0.89)
rs9378200	6	31680906	*BAT2*	C/T	0.17	0.92 (0.82–1.04)	0.59 (0.52–0.67)
rs9271731	6	32701590	*HLA–DRB1–HLA–DQA1*	G/A	0.41	1.06 (0.92–1.22)	1.34 (1.25–1.45)
rs9469220	6	32766288	*HLA–DQA1*	A/G	0.027	0.88 (0.78–0.98)	0.65 (0.61–0.68)

* SLE = systemic lupus erythematosus (see Table 2 for other definitions).
† For ANA positivity.
‡ For SLE susceptibility.

sible for self recognition and antigen presentation, the association between the polymorphisms in the HLA locus and ANAs seemed reasonable. HLA–DRB1*0405 is associated with a wide range of rheumatic and autoimmune diseases (26,31). This raised the possibility that autoimmune-related markers also had effects on ANA production. We selected SLE as being representative of autoimmune diseases with ANA production, and we analyzed the effects of a total of 7 markers that were reported to be associated with SLE in a previous Japa-

Table 4. Associations of ANA positivity with imputed HLA–DRB1 and HLA–DQB1 alleles*

HLA allele	Model	*P*	Corrected *P*†	OR (95% CI)	Accuracy
HLA–DRB1					
DRB1*0405	Dominant	3.0×10^{-5}	0.00081	1.43 (1.21–1.70)	0.902
DRB1*1302	Additive	3.6×10^{-5}	0.00097	0.69 (0.58–0.82)	0.997
DRB1*1201	Additive	0.00021	0.0057	0.58 (0.44–0.78)	0.704
DRB1*1401	Additive	0.069	1	0.80 (0.62–1.02)	0.746
DRB1*1101	Additive	0.095	1	0.77 (0.57–1.05)	0.827
DRB1*0901	Additive	0.11	1	1.13 (0.97–1.31)	1
DRB1*0701	Additive	0.23	1	0.37 (0.07–1.89)	1
DRB1*0803	Additive	0.33	1	1.10 (0.91–1.33)	0.987
DRB1*1502	Additive	0.52	1	0.95 (0.82–1.11)	0.998
DRB1*0401	Dominant	0.58	1	1.12 (0.74–1.71)	0.883
DRB1*1501	Additive	0.66	1	1.05 (0.86–1.28)	0.992
DRB1*1001	Additive	0.67	1	0.86 (0.42–1.74)	0.909
DRB1*1202	Additive	0.69	1	0.93 (0.64–1.34)	0.964
DRB1*0802	Additive	0.74	1	1.05 (0.77–1.45)	0.808
DRB1*0101	Dominant	0.90	1	1.01 (0.82–1.25)	0.992
HLA–DQB1					
DQB1*0301	Additive	3.5×10^{-5}	0.00095	0.71 (0.61–0.84)	0.888
DQB1*0604	Additive	0.00027	0.0073	0.71 (0.60–0.86)	1
DQB1*0401	Dominant	0.00031	0.0084	1.38 (1.16–1.65)	0.902
DQB1*0302	Dominant	0.0087	0.24	1.30 (1.07–1.59)	1
DQB1*0503	Additive	0.087	1	0.78 (0.58–1.04)	1
DQB1*0303	Additive	0.11	1	1.13 (0.97–1.31)	0.819
DQB1*0201	Dominant	0.15	1	3.46 (0.65–18.39)	1
DQB1*0402	Additive	0.20	1	1.18 (0.92–1.51)	0.907
DQB1*0602	Additive	0.49	1	1.08 (0.87–1.32)	1
DQB1*0601	Dominant	0.67	1	0.97 (0.83–1.12)	1
DQB1*0502	Dominant	0.75	1	0.95 (0.67–1.34)	1
DQB1*0501	Dominant	0.89	1	1.01 (0.83–1.24)	1

* See Table 2 for definitions.
† Corrected by Bonferroni adjustment.

nese study (15). The genotypes of these 7 markers were imputed using subjects in the Nagahama Study genotyped by denser arrays as a reference. All of the alleles showed good quality of imputation ($R^2 > 0.95$), but none of them displayed strong associations with ANA positivity ($P > 0.01$) (Table 3).

Since the HLA locus, especially HLA–DRB1, is the established locus for susceptibility to SLE with multiple independent associations shown beyond ethnicity (15,28,32), we analyzed detailed associations between the HLA locus and ANA positivity. A previous European study identified 5 independent SNPs that confer susceptibility to SLE (28). Because 1 of the 5 SNPs (rs1150703) is monomorphic in Japanese, the results for 4 SNPs are given in the current study (Table 3). None of them showed comparable associations in Europeans. We also performed imputation of HLA–DRB1 and HLA–DQB1 alleles (see Subjects and Methods). While the previous European study suggested the independent association of HLA–DQA1*0102 with SLE, we used HLA–DRB1*1501 and *1302 instead, which explained large parts of the association between HLA–DQA1*0102 and SLE (28). HLA–DRB1*0405, which was moderately tagged by rs2395185, showed a positive association with the smallest P value ($P_{corr} = 0.00081$) (Table 4). HLA–DQB1*0401 also showed a positive association, and HLA–DRB1*1302 and *1201 and HLA–DQB1*0301 and *0604 showed negative associations ($P_{corr} \leq 0.0084$) (Table 4). The associations of HLA–DQB1*0401, *0604, and *0301 seemed to be explained with HLA–DRB1*0405, HLA–DRB1*1302, and a combination of HLA–DRB1*1201 and HLA–DRB1*1101, respectively (r^2 values of 0.99, 0.92, and 0.59, respectively). HLA–DRB1*1501, the strongest susceptibility allele in Japanese (32), did not show a significant association (Table 4).

Considering the negative association of HLA–DRB1*1302 and the lack of association of HLA–DRB1*1501, HLA–DQA1*0102 was assumed to display a suggestive negative association. HLA–DRB1*0901, *0802, and *0401, which showed independent significant positive associations with SLE in Japanese (32), were not associated with ANA positivity.

Next, we addressed the similarities and differences of associations in the HLA locus among ANA staining patterns. Among the 2,820 SNPs in the HLA locus, rs9368726 and rs1964995, both of which were in strong LD with rs2395185 (r^2 values of 1.0 and 0.72, respectively), showed the strongest associations with speckled and homogeneous patterns, respectively ($P = 1.1 \times 10^{-7}$ and $P = 3.6 \times 10^{-8}$, respectively, in the GWAS) (Figure 2A). When we used the genotyping

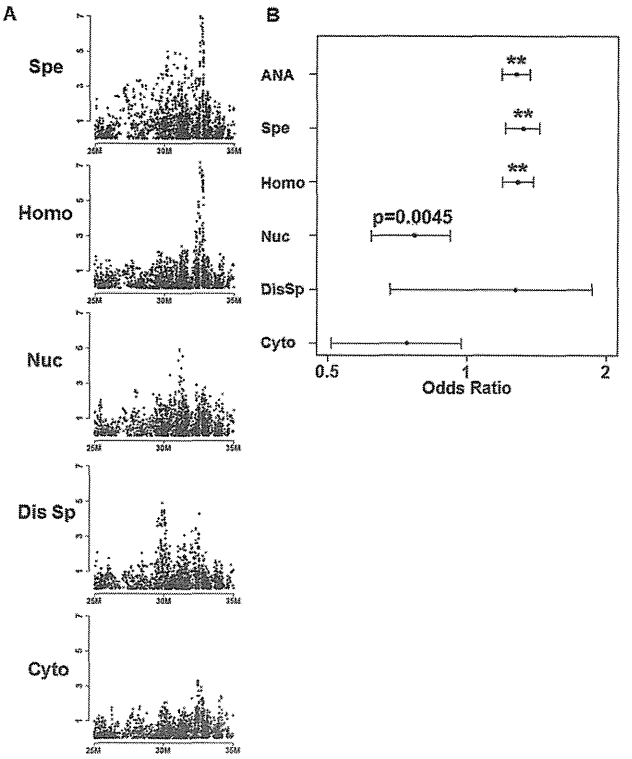

Figure 2. Heterogeneous association of the HLA locus among staining patterns of antinuclear antibodies (ANAs). **A,** Regional Manhattan plots for different staining patterns in the HLA region. **B,** Odds ratios and 95% confidence intervals of associations between rs2395185 and ANAs or their staining patterns. ** = $P < 1.0 \times 10^{-10}$. Spe = speckled; Homo = homogeneous; Nuc = nucleolar; Dis Sp = discrete speckled; Cyto = cytoplasmic.

results of rs2395185 instead of the 2 SNPs, the associations were also observed in the replication study (overall $P = 7.5 \times 10^{-12}$ and overall $P = 2.2 \times 10^{-11}$ for speckled and homogeneous patterns, respectively) (Table 2). The strongest associations with nucleolar and discrete speckled patterns in the HLA locus were observed for rs6457300 and rs1611185, respectively (both $P = 1.2 \times 10^{-5}$) (Table 2). Both SNPs are located >1.4 Mb from rs2395185. The cytoplasmic pattern showed the strongest association with rs9268347 ($P = 0.00052$), which is located 101 kb from rs2395185. We further genotyped rs6457300 and rs1611185 in the replication study, but the associations were not replicated (Table 2).

We focused on rs2395185 since it was the only SNP that demonstrated increasing effects on speckled and homogeneous patterns beyond levels significant in GWAS. Despite its increasing effects on the production of speckled and homogeneous patterns, the SNP displayed a significant decreasing effect on the nucleolar

pattern ($P = 0.0045$) (Figure 2B). Next, we analyzed whether rs2395185 had increasing effects on ANA levels in subjects positive for ANAs. When we examined subjects with ANA titers ≥1:40 and reviewed the staining patterns, the T allele of rs2395185 showed suggestive or significant increasing effects on levels of total, speckled, and homogeneous patterns ($P = 0.12$, $P = 0.016$, and $P = 0.00030$, respectively, by Jonckheere-Terpstra test).

DISCUSSION

The current study provided solid evidence of the distribution and correlates of ANAs in a Japanese adult population. This is the first study to perform GWAS of ANAs in healthy populations and detect a significant locus. The nucleolar pattern has characteristics that differ from those of other staining patterns. Autoantibodies such as anti–U3 RNP, anti-Th/To, or antiribosomal antibodies, associated with systemic sclerosis or SLE, are classified as having the nucleolar pattern of ANAs.

In our study, 12.5% of healthy participants had ANA titers of ≥1:80, which is comparable to previous results in the US (4,754 individuals, 13.8%) (14). The percentages were slightly higher than in previous studies for the cutoff level of 1:40 and comparable for the cutoff level of 1:160 (~26.8–31.7% and ~5.0–8.1%, respectively, in previous studies). Of the 201 subjects who were excluded due to the possibility of having autoimmune diseases, 141 had ANA titers of ≥1:40 (70.1%) (data not shown), suggesting the validity of the exclusion criteria. The increase in ANA positivity in women was confirmed, and this association could partly be explained by sex hormones (33–35). Considering the sex difference in onset of autoimmune diseases, the same undetermined mechanisms related to sex may underlie ANA production in healthy populations.

This study showed a strong effect of age on positivity for ANAs. We did not observe an increase in positivity for ANAs with aging in subjects 30–50 years old ($P = 0.20$) (data not shown); therefore, the elderly populations largely accounted for the association between aging and ANA positivity. The increase in ANAs after age 50 years matches the results in the US study. This association might be explained by dysregulation of immunologic tolerance in the elderly population. Considering the previous reports of high ANA levels in the adolescent population (13,36), the association between ANA positivity and aging in the general population seems to have a "U" pattern (lowest ANA levels at ages with most frequent reproduction). The effects of age and sex on ANAs seemed to differ among the staining patterns. The nucleolar pattern did not display significant associations with age and sex. As discrete speckled patterns showed positive associations, the lack of association of the nucleolar pattern with age and sex cannot be explained by its frequency.

Correlates of ANAs seemed to partly differ between different populations. The current study did not find a significant association between obesity and ANA positivity. However, obesity tended to be inversely related to ANA positivity as in the US study, and the limited number of obese individuals in the current study might explain this nonsignificant association. The association between increased CRP levels and ANA positivity was not found in the previous study. Chronic mild inflammation would lead to the production of ANAs. Since the distribution of CRP levels in subjects differs greatly between the 2 studies, further analysis would clarify the association.

The current study identified rs2395185 in the HLA class II locus as a marker of susceptibility to ANA positivity. It should be noted that a previous study showed an association between rs2395185 and ulcerative colitis (37), suggesting the involvement of rs2395185 with autoimmune processes. Because a previous study showed that the type I interferon (IFN) signature is up-regulated in healthy populations with high ANA titers (38), it will be interesting to analyze the functional roles of rs2395185 in the type I IFN pathway.

The T allele of rs2395185 showed increasing effects on levels of speckled and homogeneous patterns, but a decreasing effect on levels of the nucleolar pattern. This indicates that the nucleolar pattern also differs from the speckled and homogeneous patterns in terms of HLA association. The detailed plots in the HLA locus support the notion of different association patterns among ANA staining patterns. The opposing effect of rs2395185 on levels of the nucleolar pattern indicates that the lack of common association of rs2395185 over staining patterns of ANAs was not due to lower positivity for several staining patterns. As the HLA class II locus is strongly associated with presentation and recognition of antigen, the current results may suggest that ANA production is associated with binding affinity of antigens to the HLA molecule. Since antigens recognized by ANAs contain a wide variety of molecules, the common strong association of 1 polymorphism with speckled and homogeneous patterns suggests similarity or cross-reactivity of antigens that correspond to speckled or homogeneous patterns. The opposing effect also suggests that antigens corresponding to the nucleolar pattern are not presented by common HLA class II alleles with speckled and homogeneous patterns.

As HLA–DRB1*0405 is associated with susceptibility to immunologic disorders or autoantibody production in autoimmune diseases (27,39), the association between ANA production and rs2395185 in LD with HLA–DRB1*0405 might suggest a common mechanism between HLA–DRB1*0405–related autoimmune disease susceptibility and production of ANAs. At the same time, the association raises the possibility that genes conferring susceptibility to ANA positivity might be identified as genes conferring susceptibility to connective tissue diseases.

However, the current study did not detect significant associations between SLE-related SNPs or HLA alleles and ANA positivity. These results indicated that SNPs significantly associated with SLE in the previous study were associated with SLE itself and not with ANAs. Lack of association between ANA production in healthy subjects and rs9501626 or HLA–DRB1*1501, the most significant HLA SNP or HLA–DRB1 allele associated with SLE in the Japanese population, may suggest that autoantigens recognized by ANAs in SLE patients are different from those recognized by ANAs in healthy populations. In fact, a previous study showed that healthy subjects with high ANA titers exhibited an autoantibody profile distinct from that in SLE patients (38). These results may also suggest the involvement of immunologic molecular pathways in SLE development that are not related to ANA production in healthy populations. While we did not find associations of the 7 SNPs in Japanese and the 4 SNPs in Europeans, we observed that 9 of the 11 SNPs had a common direction of association between SLE susceptibility and ANA positivity. All the susceptibility DRB1 alleles in Japanese (HLA–DRB1*1501, *0901, *0802, and *0401) also showed a trend toward increasing ANAs. The common directionality between SLE susceptibility and ANA positivity may be meaningful.

It will be interesting to finely genotype the HLA locus to determine the polymorphisms and mechanisms responsible for causing the associations with ANAs or speckled and homogeneous patterns. None of the polymorphisms display significant associations with nucleolar, discrete speckled, or cytoplasmic patterns. However, considering the low positivity for these staining patterns and the strength of associations in the HLA locus in the current study, increasing the number of subjects would identify yet-to-be-determined polymorphisms associated with these staining patterns. We did not observe significant associations with ANA positivity outside the HLA locus. In addition, none of the polymorphisms outside the HLA locus showed suggestive associations with ANA staining patterns (data not shown). The significance and roles of ANAs in healthy populations have not yet been clarified. Because a previous study showed that the type I IFN signature is up-regulated in healthy populations with high ANA titers (38), it is possible that high ANA titers in healthy populations reflect a pre–autoimmune disease state. Further followup and analyses are necessary to address these points.

Taken together, the current study determined that the HLA class II locus is a locus for susceptibility to ANA production. Genetic overlap between SLE susceptibility and ANA production in healthy populations is limited. The current results indicate that ANAs are not homogeneous autoantibodies with similar characteristics. It is feasible to analyze whether the current results are observed in different populations, especially in Europeans.

ACKNOWLEDGMENTS

We are grateful to the Nagahama City Office and the nonprofit organization Zeroji Club for their help in performing the Nagahama Study.

AUTHOR CONTRIBUTIONS

All authors were involved in drafting the article or revising it critically for important intellectual content, and all authors approved the final version to be published. Dr. Terao had full access to all of the data in the study and takes responsibility for the integrity of the data and the accuracy of the data analysis.

Study conception and design. Terao, Ohmura, Yamada, Kawaguchi, Shimizu, Tabara, Takahashi, Setoh, Nakayama, Kosugi, Sekine, Matsuda, Mimori.

Acquisition of data. Terao, Ohmura, Yamada, Kawaguchi, Shimizu, Tabara, Takahashi, Setoh, Nakayama, Kosugi, Sekine, Matsuda, Mimori.

Analysis and interpretation of data. Terao, Kawaguchi.

REFERENCES

1. Czaja AJ, Nishioka M, Morshed SA, Hachiya T. Patterns of nuclear immunofluorescence and reactivities to recombinant nuclear antigens in autoimmune hepatitis. Gastroenterology 1994; 107:200–7.
2. Solomon DH, Kavanaugh AJ, Schur PH, and the American College of Rheumatology Ad Hoc Committee on Immunologic Testing Guidelines. Evidence-based guidelines for the use of immunologic tests: antinuclear antibody testing. Arthritis Rheum 2002;47:434–44.
3. Petri M, Karlson EW, Cooper DS, Ladenson PW. Autoantibody tests in autoimmune thyroid disease: a case-control study. J Rheumatol 1991;18:1529–31.
4. Rich S, Kieras K, Hart K, Groves BM, Stobo JD, Brundage BH. Antinuclear antibodies in primary pulmonary hypertension. J Am Coll Cardiol 1986;8:1307–11.
5. Guyomard S, Salles G, Coudurier M, Rousset H, Coiffier B, Bienvenu J, et al. Prevalence and pattern of antinuclear autoantibodies in 347 patients with non-Hodgkin's lymphoma. Br J Haematol 2003;123:90–9.
6. Bonnet F, Pineau JJ, Taupin JL, Feyler A, Bonarek M, de Witte S, et al. Prevalence of cryoglobulinemia and serological markers of

autoimmunity in human immunodeficiency virus infected individuals: a cross-sectional study of 97 patients. J Rheumatol 2003;30: 2005–10.
7. Koenig M, Dieude M, Senecal JL. Predictive value of antinuclear autoantibodies: the lessons of the systemic sclerosis autoantibodies. Autoimmun Rev 2008;7:588–93.
8. Buyon JP, Ben-Chetrit E, Karp S, Roubey RA, Pompeo L, Reeves WH, et al. Acquired congenital heart block: pattern of maternal antibody response to biochemically defined antigens of the SSA/Ro-SSB/La system in neonatal lupus. J Clin Invest 1989;84:627–34.
9. Hahn BH. Antibodies to DNA. N Engl J Med 1998;338:1359–68.
10. Tan EM, Feltkamp TE, Smolen JS, Butcher B, Dawkins R, Fritzler MJ, et al. Range of antinuclear antibodies in "healthy" individuals. Arthritis Rheum 1997;40:1601–11.
11. Petri M, Orbai AM, Alarcon GS, Gordon C, Merrill JT, Fortin PR, et al. Derivation and validation of the Systemic Lupus International Collaborating Clinics classification criteria for systemic lupus erythematosus. Arthritis Rheum 2012;64:2677–86.
12. Alvarez F, Berg PA, Bianchi FB, Bianchi L, Burroughs AK, Cancado EL, et al. International Autoimmune Hepatitis Group Report: review of criteria for diagnosis of autoimmune hepatitis. J Hepatol 1999;31:929–38.
13. Hayashi N, Koshiba M, Nishimura K, Sugiyama D, Nakamura T, Morinobu S, et al. Prevalence of disease-specific antinuclear antibodies in general population: estimates from annual physical examinations of residents of a small town over a 5-year period. Mod Rheumatol 2008;18:153–60.
14. Satoh M, Chan EK, Ho LA, Rose KM, Parks CG, Cohn RD, et al. Prevalence and sociodemographic correlates of antinuclear antibodies in the United States. Arthritis Rheum 2012;64:2319–27.
15. Okada Y, Shimane K, Kochi Y, Tahira T, Suzuki A, Higasa K, et al. A genome-wide association study identified AFF1 as a susceptibility locus for systemic lupus erythematosus in Japanese. PLoS Genet 2012;8:e1002455.
16. Terao C, Yamada R, Ohmura K, Takahashi M, Kawaguchi T, Kochi Y, et al. The human AIRE gene at chromosome 21q22 is a genetic determinant for the predisposition to rheumatoid arthritis in Japanese population. Hum Mol Genet 2011;20:2680–5.
17. Terao C, Ohmura K, Katayama M, Takahashi M, Kokubo M, Diop G, et al. Myelin basic protein as a novel genetic risk factor in rheumatoid arthritis—a genome-wide study combined with immunological analyses. PLoS One 2011;6:e20457.
18. Terao C, Yoshifuji H, Kimura A, Matsumura T, Ohmura K, Takahashi M, et al. Two susceptibility loci to Takayasu arteritis reveal a synergistic role of the IL12B and HLA-B regions in a Japanese population. Am J Hum Genet 2013;93:289–97.
19. Kamatani Y, Matsuda K, Okada Y, Kubo M, Hosono N, Daigo Y, et al. Genome-wide association study of hematological and biochemical traits in a Japanese population. Nat Genet 2010;42: 210–5.
20. Schur PH, Sandson J. Immunologic factors and clinical activity in systemic lupus erythematosus. N Engl J Med 1968;278:533–8.
21. Koffler D, Agnello V, Winchester R, Kunkel HG. The occurrence of single-stranded DNA in the serum of patients with systemic lupus erythematosus and other diseases. J Clin Invest 1973;52: 198–204.
22. Yoshimura K, Nakayama T, Sekine A, Matsuda F, Kosugi S, Sugino Y, et al, and the Nagahama Cohort Research Group. Prevalence of postmicturition urinary incontinence in Japanese men: comparison with other types of incontinence. Int J Urol 2013;20:911–6.
23. Terao C, Ohmura K, Ikari K, Kawaguchi T, Takahashi M, Setoh K, et al, on behalf of the Nagahama Study Group. The effects of smoking and shared epitope on the production of ACPA and RF in a Japanese adult population: the Nagahama Study. Arthritis Care Res (Hoboken) 2014. E-pub ahead of print.
24. Devlin B, Roeder K. Genomic control for association studies. Biometrics 1999;55:997–1004.
25. Dilthey A, Leslie S, Moutsianas L, Shen J, Cox C, Nelson MR, et al. Multi-population classical HLA type imputation. PLoS Comput Biol 2013;9:e1002877.
26. Terao C, Ohmura K, Kochi Y, Ikari K, Maruya E, Katayama M, et al. A large-scale association study identified multiple HLA-DRB1 alleles associated with ACPA-negative rheumatoid arthritis in Japanese subjects. Ann Rheum Dis 2011;70:2134–9.
27. Terao C, Ikari K, Ohmura K, Suzuki T, Iwamoto T, Takasugi K, et al. Quantitative effect of HLA-DRB1 alleles to ACPA levels in Japanese rheumatoid arthritis: no strong genetic impact of shared epitope to ACPA levels after stratification of HLA-DRB1*09:01. Ann Rheum Dis 2012;71:1095–7.
28. Morris DL, Taylor KE, Fernando MM, Nititham J, Alarcon-Riquelme ME, Barcellos LF, et al. Unraveling multiple MHC gene associations with systemic lupus erythematosus: model choice indicates a role for HLA alleles and non-HLA genes in Europeans. Am J Hum Genet 2012;91:778–93.
29. Li Y, Willer CJ, Ding J, Scheet P, Abecasis GR. MaCH: using sequence and genotype data to estimate haplotypes and unobserved genotypes. Genet Epidemiol 2010;34:816–34.
30. Purcell S, Neale B, Todd-Brown K, Thomas L, Ferreira MA, Bender D, et al. PLINK: a tool set for whole-genome association and population-based linkage analyses. Am J Hum Genet 2007; 81:559–75.
31. Yamashita H, Awata T, Kawasaki E, Ikegami H, Tanaka S, Maruyama T, et al, on behalf of the Japanese Study Group on Type 1 Diabetes Genetics. Analysis of the HLA and non-HLA susceptibility loci in Japanese type 1 diabetes. Diabetes Metab Res Rev 2011;27:844–8.
32. Shimane K, Kochi Y, Suzuki A, Okada Y, Ishii T, Horita T, et al. An association analysis of HLA-DRB1 with systemic lupus erythematosus and rheumatoid arthritis in a Japanese population: effects of *09:01 allele on disease phenotypes. Rheumatology (Oxford) 2013;52:1172–82.
33. Nashold FE, Spach KM, Spanier JA, Hayes CE. Estrogen controls vitamin D_3-mediated resistance to experimental autoimmune encephalomyelitis by controlling vitamin D_3 metabolism and receptor expression. J Immunol 2009;183:3672–81.
34. Wilder RL. Neuroendocrine-immune system interactions and autoimmunity. Annu Rev Immunol 1995;13:307–38.
35. Strickland FM, Hewagama A, Lu Q, Wu A, Hinderer R, Webb R, et al. Environmental exposure, estrogen and two X chromosomes are required for disease development in an epigenetic model of lupus. J Autoimmun 2012;38:J135–43.
36. Yoshida H, Imafuku Y, Morita EO, Nagai T, Kato Y, Motegi S. Detection of antinuclear antibodies and their significance as disease markers. Rinsho Byori 1994;42:455–9. In Japanese.
37. Silverberg MS, Cho JH, Rioux JD, McGovern DP, Wu J, Annese V, et al. Ulcerative colitis-risk loci on chromosomes 1p36 and 12q15 found by genome-wide association study. Nat Genet 2009; 41:216–20.
38. Li QZ, Karp DR, Quan J, Branch VK, Zhou J, Lian Y, et al. Risk factors for ANA positivity in healthy persons. Arthritis Res Ther 2011;13:R38.
39. Terao C, Ohmura K, Ikari K, Kochi Y, Maruya E, Katayama M, et al. ACPA-negative RA consists of two genetically distinct subsets based on RF positivity in Japanese. PLoS One 2012;7: e40067.

Association of Serum–Free Fatty Acid Level With Reduced Reflection Pressure Wave Magnitude and Central Blood Pressure

The Nagahama Study

Yasuharu Tabara, Yoshimitsu Takahashi, Takahisa Kawaguchi, Kazuya Setoh, Chikashi Terao, Ryo Yamada, Shinji Kosugi, Akihiro Sekine, Takeo Nakayama, Fumihiko Matsuda, on behalf of the Nagahama Study Group

Abstract—Central blood pressure (BP) has been suggested to be a better predictor of cardiovascular disease risk than brachial BP. Given that central BP and arterial waveform are both influenced by insulin resistance, major initiators of insulin resistance, such as serum–free fatty acid (FFA), are suspected of potentially being involved in central hemodynamics. To confirm that insulin signaling is an important modulator of central hemodynamics, we investigated this hypothesis in a large-scale general population. Brachial BP and radial arterial waveform were measured simultaneously in 9393 middle-aged to elderly individuals. The augmentation index was calculated from the radial waveform as the ratio of the height of the late systolic peak to that of the first peak. Central systolic BP was defined as the absolute pressure of the late systolic peak of the waveform. Differences in central and brachial pulse pressure (PP) were considered to represent PP amplification. PP amplification differed significantly among serum FFA level quartiles (Q1, 7.8±5.3; Q2, 8.6±5.0; Q3, 9.3±5.7; Q4, 10.3±6.1 mm Hg; $P<0.001$), and the maximum difference in combination with diabetes mellitus status was 4.9 mm Hg. Multivariate analysis adjusted for major covariates indicated that higher serum FFA was an independent determinant for higher PP amplification ($\beta=0.145$, $P<0.001$) and lower augmentation index ($\beta=-0.122$, $P<0.001$) and central systolic BP ($\beta=-0.044$, $P<0.001$), whereas the association between FFA and PP amplification significantly decreased ($\beta=0.022$, $P<0.001$) after further adjustment for augmentation index. Serum FFA is an overlooked factor favorably influencing central hemodynamics. A low-magnitude reflection pressure wave might be involved in this paradoxical relationship. (***Hypertension*. 2014;64:1212-1218.**) • **Online Data Supplement**

Key Words: aortic blood pressure ■ free fatty acid ■ insulin resistance ■ pulse wave analysis

Hypertension is a leading cause of cardiovascular disease, with brachial blood pressure (BP) being a standard measure in the assessment of arterial pressure load. However, central BP estimated from the radial arterial waveform has recently been suggested to be more closely associated with cardiovascular outcomes than brachial BP.[1–3] In addition to these epidemiological findings, clinical studies from several groups[4–6] and our own[7] have suggested that antihypertensive drugs might exert different effects on arterial waveform and central BP, possibly resulting in different cardiovascular outcomes. The Conduit Artery Function Evaluation substudy[4] of the Anglo-Scandinavian Cardiac Outcomes Trial demonstrated that calcium channel blockers were superior to β-blockers for reducing cardiovascular events. This effect was presumably because of the central systolic BP (SBP) being lower in the calcium channel blocker treatment arm, whereas no class-specific effects were observed regarding brachial SBP. The apparent influence of central BP on cardiac outcomes highlights the importance of identifying factors that might affect central BP levels.

Several factors have been reported to influence central BP levels by altering the arterial pressure waveform,[8] a composite waveform of the forward pressure wave generated by cardiac ejection and the backward pressure wave reflected at peripheral sites. Arterial stiffness causes the early return of reflection pressure waves from peripheral sites and thus increases overlaps between forward and reflection pressure waves at the aorta, which increase central SBP. Other factors also influence arterial waveform, such as tall stature greatly decreasing the overlap of the 2 waveforms by delaying the arrival of the

Received July 25, 2014; first decision August 3, 2014; revision accepted August 21, 2014.

From the Center for Genomic Medicine, Kyoto University Graduate School of Medicine, Kyoto, Japan (Y.T., T.K., K.S., C.T., R.Y., F.M.); Departments of Health Informatics (Y.T., T.N.) and Medical Ethics and Medical Genetics (S.K.), Kyoto University School of Public Health, Kyoto, Japan; and Kyoto University Medical Research Support Center, Kyoto, Japan (A.S.).

The online-only Data Supplement is available with this article at http://hyper.ahajournals.org/lookup/suppl/doi:10.1161/HYPERTENSIONAHA.114.04277/-/DC1.

Correspondence to Yasuharu Tabara, Center for Genomic Medicine, Kyoto University Graduate School of Medicine, Shogoinkawaramachi 53, Sakyo-ku, Kyoto 606–8507, Japan. E-mail tabara@genome.med.kyoto-u.ac.jp

Hypertension **is available at http://hyper.ahajournals.org** **DOI: 10.1161/HYPERTENSIONAHA.114.04277**

reflection pressure wave and increased heart rate (HR) reducing the overlap by shortening the cardiac ejection period.

Curiously, type 2 diabetes mellitus and insulin resistance have been favorably associated with central hemodynamics. Several groups[9,10] and our own[11] have shown that individuals with type 2 diabetes mellitus had relatively low central SBP, despite the well-established pathogenicity of diabetes mellitus for arterial stiffness and cardiovascular diseases. Although the mechanisms behind this paradoxical relationship are unclear, a possible explanation is reduced magnitude of the reflection pressure wave[12] because of a stiffer aortic artery and consequently larger penetration of pulsatile energy into the microcirculation.[13,14] Insulin-mediated vasoconstriction under insulin-resistant conditions[15] might also be involved in the increased transmission of pulsatile energy.

Free fatty acid (FFA) is a major initiator of insulin resistance.[15,16] FFA blocks insulin signaling via phosphorylation of insulin receptor substrate 1, which inhibits translocation of glucose transporter to the cell membrane and reduces glucose uptake.[15] Further, FFA has been shown to reduce endothelium-dependent vasodilation by decreasing endothelial nitric oxide production.[14] Given these molecular bases of FFA in initiation of insulin resistance, we hypothesized that serum FFA levels might also be associated with central hemodynamics. Proving our hypothesis would further support the involvement of insulin signaling in central hemodynamic control and would help to further understand the basis of paradoxical relationship between insulin resistance and better central hemodynamic profile.

Here, we investigated our hypothesis using a data set from the Nagahama Prospective Cohort for Comprehensive Human Bioscience (the Nagahama Study), a large-scale population-based cohort study in Japan.

Methods

Study Subjects

Study subjects were 9393 apparently healthy middle-aged to elderly citizens who had participated in the Nagahama Study. This study cohort was recruited from 2008 to 2010 from the general population of Nagahama City, a largely suburban city of 125 000 inhabitants in central Japan. Community residents aged 30 to 74 years, living independently and with no physical impairment or dysfunction, were recruited. Of 9804 total subjects, those meeting any of the following conditions were excluded from this study: history of symptomatic cardiovascular diseases (n=266), taking insulin therapy (n=22), unsuccessful assessment of clinical parameters required for this study (n=80), and pregnant women (n=43).

Of the 9393 subjects remaining after exclusion, individuals with available fasting blood specimens (>11 hours) were used as the study panel (n=4322), whereas those with peripheral blood samples drawn within 10 hours of their last meal were used as the replication panel (n=5071).

All study procedures were approved by the ethics committee of Kyoto University Graduate School of Medicine and the Nagahama Municipal Review Board. Written informed consent was obtained from all participants.

BP Measurement

Radial arterial waveform, brachial BP, and HR were measured simultaneously (HEM-9000AI; Omron Healthcare, Kyoto, Japan) after 5 minutes resting in the sitting position. Briefly, brachial BP was measured at the right upper arm using a cuff-oscillometric device, and the radial arterial waveform was simultaneously obtained from the left wrist using a multielement tonometry sensor. The augmentation index (AIx) was calculated from the radial arterial waveform as the ratio of the height of the late systolic peak (SBP2) to the first systolic peak. The absolute pressure of SBP2 obtained by calibrating the first systolic peak with brachial SBP was considered to represent the central SBP. Pulse pressure (PP) amplification was calculated by subtracting central PP from brachial PP and expressed in absolute values (mm Hg). Measurements were taken twice, and the mean value of these measurements was used in analysis. The validity of SBP2 in estimating central SBP has been demonstrated by invasive simultaneous measurement of the ascending aorta and radial artery pressure.[17,18] We also previously reported that radial SBP2 was closely related to the central SBP calculated by the widely used generalized transfer function.[19] Mean BP was calculated using the following formula: Mean BP=diastolic BP +(SBP−diastolic BP)/3.

Clinical Parameters

Basic clinical parameters were measured at the baseline examination of the Nagahama cohort study. Serum FFA levels were quantified using an enzymatic assay (NEFA-HR; Wako Pure Chemical Industries, Ltd., Osaka, Japan). Intra- and interassay coefficients of variation in FFA measurements were 1.42% and 1.79%, respectively. Homeostasis model assessment of insulin resistance was calculated as an index of insulin resistance using the following formula: [insulin (IU/l)×glucose (mg/dL)]/405.

Assessment of Arterial Stiffness

Arterial stiffness was assessed by pulse wave velocity (PWV) measured between the brachia and ankle (baPWV). Briefly, cuffs were applied to both brachia and ankles, and BP was measured simultaneously in the supine position using a cuff-oscillometric device (Vasera-1500; Fukuda Denshi, Tokyo, Japan). Pulse volume waveforms were also recorded simultaneously using a plethysmographic sensor connected to the cuffs. The baPWV was calculated from the time interval between the wave fronts of the brachial and ankle waveforms and the path length from the brachia to ankle (0.597×height+14.4014).[20] The colinearity of baPWV with a carotid-to-femoral PWV, a standard measure of arterial stiffness, has been previously reported.[21]

Statistical Analysis

Quartile of PP amplification and serum FFA level was calculated for each sex and then combined to avoid potential sex differences. Differences in numeric parameters among subgroups were assessed by analysis of variance, whereas the frequency of differences among subgroups was evaluated using a χ^2 test. Factors independently associated with PP amplification and AIx were assessed by multiple linear regression analysis. Statistical analysis was performed using JMP 9.0.3 software (SAS Institute, Cary, NC, USA). $P<0.05$ indicated statistical significance.

Results

Clinical characteristics of study subjects are summarized in Table 1. Plasma levels of triglycerides, insulin, and FFA were slightly higher in the replication panel than in the study panel ($P<0.001$), whereas no marked differences were observed for other parameters.

Table 2 shows the differences in metabolic parameters among quartiles of PP amplification. Subjects with larger PP amplification were markedly younger and taller and had faster HR than those with less amplification. Although several clinical parameters significantly differed among quartiles in crude analysis, parameters for insulin resistance, including FFA levels, remained significant even after adjustment for major covariates.

As a whole, women had significantly higher FFA levels than men (Figure 1). Older age ($r=0.087$, $P<0.001$), lower body mass index ($r=-0.084$, $P<0.001$), increased high-density lipoprotein

Table 1. Clinical Characteristics of Study Subjects

Factors	Study Panel (4322)	Replication Panel (5071)
Age, y	53±13	53±13
Sex (men, %)	31.6	32.9
Body height, cm	160.1±8.4	159.9±8.5
Body weight, kg	57.0±10.9	57.3±10.9
Body mass index, kg/m^2	22.1±3.2	22.4±3.3
Waist circumference, cm*	79.8±9.8	80.4±9.3
Medication, %		
Hypertension	15.6	16.1
Hyperglycemia	2.4	2.4
Dyslipidemia	11.5	10.9
Brachial SBP, mm Hg	123±18	124±18
Central SBP, mm Hg	114±19	114±18
DBP, mm Hg	76±11	76±11
PP amplification, mm Hg	9±6	10±6
Radial AIx, %	81.6±13.4	79.8±13.4
Heart rate, bpm	69±10	70±10
baPWV, cm/s	1261±231	1262±227
Type 2 diabetes mellitus	4.0	3.6
Glucose, mg/dL	90±14	90±16
HbA1c, %	5.5±0.5	5.4±0.5
Insulin, μU/mL	5.0±3.1	5.7±6.1
Total cholesterol, mg/dL	207±34	207±35
HDL cholesterol, mg/dL	66±17	65±17
LDL cholesterol, mg/dL	123±31	123±31
Triglyceride, mg/dL	91±58	103±68
FFA, mEq/L	0.69±0.24	0.78±0.31

Values are mean±standard deviation. The study panel consisted of individuals whose fasting blood specimens (>11 h) were available, and the replication panel consisted of individuals whose peripheral blood samples were drawn within 10 h of their last meal. AIx indicates augmentation index; baPWV, brachial-to-ankle pulse wave velocity; DBP, diastolic blood pressure; FFA, free fatty acid; HbA1c, hemoglobin A1c; HDL, high-density lipoprotein; LDL, low-density lipoprotein; PP, pulse pressure; and SBP, systolic blood pressure.

*Data available for 4320 (study panel) and 5069 (replication panel) subjects. Type 2 diabetes mellitus was defined as one or more of fasting plasma glucose ≥126 mg/dL, occasional plasma glucose ≥200 mg/dL, HbA1c ≥6.5%, or taking oral antihyperglycemic drugs.

(r=0.190, P<0.001) and total cholesterol levels (r=0.085, P<0.001), and higher brachial SBP (r=0.057, P<0.001) had a significant but weak association with serum FFA levels (Tables S1 and S2 in the online-only Data Supplement). PP amplification markedly increased with FFA quartile (Figure 2), although both brachial and central SBP also showed linear association with FFA levels (Figure S1). In combined analysis with diabetes mellitus status (Figure 2C), differences in PP amplification between the highest (diabetic individuals with highest FFA quartile) and lowest (nondiabetic controls with lowest FFA quartile) subgroups reached ≈4.9 mm Hg. In contrast, AIx exhibited an inverse association with FFA quartile (Figure 2D), whereas baPWV was positively associated with FFA quartile (Figure 2E).

Table 3 summarizes the results of multiple regression analysis for central hemodynamic parameters. Results indicated that serum FFA level was an independent positive determinant for PP amplification (Model 1). Given that FFA was also strongly and inversely associated with AIx, we further adjusted AIx in the regression analysis (Model 2). Although the association between serum FFA and PP amplification remained significant, the regression coefficient of FFA substantially decreased. Lower AIx might, therefore, be involved in the relationship between elevated serum FFA levels and elevated PP amplification. Further, FFA overtook the positive association between plasma insulin level and AIx (Models 3 and 4). Results of these regression analyses indicated that serum FFA levels rather than plasma insulin concentration is a key factor in reducing AIx in subjects with insulin resistance. Waist circumference was not identified as an independent determinant when included instead of body weight in regression Model 4 (P=0.466). The association of FFA with AIx might be independent of adiposity. Serum FFA level also showed an inverse and independent association with central SBP after adjustment for brachial SBP (Model 5).

FFA was a positive determinant for arterial tone when assessed via baPWV (Model 6). However, the associations of FFA with AIx (Model 4), as well as central pressure (Model 1, 2, and 5), were independent of baPWV, suggesting that changes in reflection magnitude rather than transit time of the reflection pressure wave might be involved in the paradoxical relationship between higher FFA and better central hemodynamic profiles.

These findings were supported in the analysis using the replication panel, irrespective of potential differences in fasting status, and no marked sex differences were found in any regression model (Table S3). When MBP was adjusted in the regression models instead of SBP, no marked changes were observed in the regression coefficients of FFA as follows: Model 2 (PP amplification), β=0.030, P<0.001; Model 4 (AIx), β=−0.115, P<0.001; Model 5 (cSBP), β=−0.016, P<0.001; and Model 6 (baPWV), β=0.073, P<0.001. Further, the association of FFA with central hemodynamic parameter was independent of glycemic control levels assessed by hemoglobin A1c: hemoglobin A1c–adjusted regression coefficients of FFA; Model 2, β=0.022, P<0.001; Model 4, β=−0.123, P<0.001; Model 5, β=−0.044, P<0.001; and Model 6, β=0.069, P<0.001.

Discussion

In the present study, we clarified that elevated serum FFA levels were strongly associated with increased PP amplification and decreased AIx, which represents relatively low central BP, in a large-scale general population sample. To our knowledge, this is the first report of a favorable association of FFA with central BP and arterial waveform, which suggests the importance of insulin signaling as a modulator of central hemodynamics. Reduced magnitude of the reflection pressure wave might be involved in this paradoxical relationship.

Insulin resistance and diabetic status have been shown to be favorably associated with AIx and central BP in observational studies in patients with diabetes mellitus[22,23] and general populations,[9,13] as well as in an experimental study using a euglycemic insulin clamp technique.[24] We also reported that not only increased insulin resistance but also reduced insulin sensitivity assessed by an oral glucose tolerance test were factors that

Table 2. Differences in Metabolic Parameters Among the Quartile of PP Amplification (Study Panel)

		Q1	Q2	Q3	Q4	*P*	
Range, mm Hg	Men	<6.5	6.5–9.9	10.0–14.4	≥14.5	Crude	Adjusted
	Women	<4.5	4.5–7.4	7.5–10.9	≥11.0		
No. of subjects		982	1143	1101	1096		
Age, y		57±11	56±12	53±13	47±14	<0.001	
Body height, cm		158.5±7.9	159.0±8.0	160.4±8.1	162.6±8.8	<0.001	
Body weight, kg		55.6±9.7	56.7±10.2	57.0±10.6	58.7±12.4	<0.001	
Brachial SBP, mm Hg		125±19	122±17	122±18	123±19	0.006	
Heart rate, bpm		64±8	67±9	70±10	74±11	<0.001	
Glucose, mg/dL		90±13	90±11	91±16	91±14	0.026	<0.001
Insulin, μU/mL		4.6±2.8	5.0±2.9	5.0±2.9	5.5±3.5	<0.001	<0.001
HOMA-IR		1.04±0.70	1.13±0.74	1.16±0.77	1.26±1.00	<0.001	<0.001
HbA1c, %		5.5±0.4	5.5±0.4	5.5±0.6	5.3±0.6	0.294	0.006
Total cholesterol, mg/dL		210±33	208±33	207±34	202±36	<0.001	0.362
HDL cholesterol, mg/dL		66±17	65±16	66±17	66±17	0.149	0.070
LDL cholesterol, mg/dL		126±30	125±30	123±31	119±32	<0.001	0.022
Triglyceride, mg/dL		91±51	93±57	90±53	90±69	0.618	0.337
FFA, mEq/L		0.63±0.23	0.68±0.23	0.71±0.24	0.74±0.25	<0.001	<0.001

Values are mean±standard deviation. Study subjects were divided into quartile by PP amplification within sex and then combined to avoid potential sex differences. Statistical significance was assessed by analysis of variance (crude model). *P* values adjusted for age, sex, body height, body weight, and use of antihyperglycemic or lipid level–lowering drugs were obtained by linear regression analyses (adjusted model). FFA indicates free fatty acid; HbA1c, hemoglobin A1c; HDL, high-density lipoprotein; HOMA-IR, homeostasis model assessment of insulin resistance; LDL, low-density lipoprotein; and SBP, systolic blood pressure.

modulate the arterial waveform and reduce central BP.[12] In the present study, however, serum FFA was a more prominent determinant of AIx than insulin. FFA initiates insulin resistance via upstream inhibition of insulin signaling in target cells, whereas increased plasma insulin levels or hyperinsulinemia are secondary responses to compensate for reduced glucose uptake under conditions of insulin resistance. The phase difference in the roles of FFA and insulin may explain the stronger association of FFA with AIx.

In stiffer arteries, the stiffness gradient from aorta to resistant artery was progressively dissipated. Decreased stiffness gradient reduces partial reflection of the forward pressure wave and increases transmission of the pulsatile energy into peripheral microcirculation, which reduces the magnitude of reflection.[14] Chirinos et al[13] recently observed selective stiffening of the aorta, but not more distal arteries, in patients with type 2 diabetes mellitus and suggested that this selective stiffening was the underlying mechanism for the paradoxical observation of a lower reflection magnitude in subjects with type 2 diabetes mellitus. Odaira et al[25] also reported that the contribution of the wave reflection to central hemodynamics might be reduced in subjects with relatively stiff arteries. Because baPWV and AIx were inversely associated with FFA quartile, that is, faster baPWV and lower AIx in higher FFA quartiles, our findings support the pulsatile energy hypothesis.

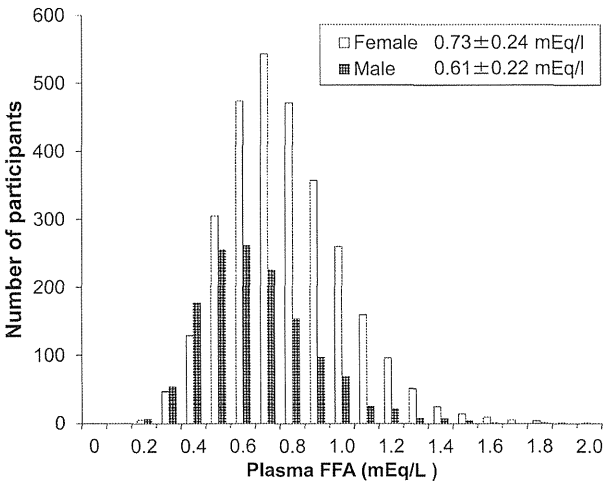

Figure 1. Histogram of serum-free fatty acid (FFA) level (study panel). Serum FFA level was significantly higher in women than in men (analysis of variance, *P*<0.001).

FFA plays a key role in the initiation of insulin resistance by inhibiting glucose uptake of target cells.[15] Given the importance of endothelium-derived nitric oxide in vascular relaxation shown in an animal model of hypertension,[26] the decreased nitric oxide production at the endothelium and subsequent endothelial dysfunction are concomitant mechanisms for the development of insulin resistance via FFA.[15] As our study participants were an apparently healthy general population without severe insulin resistance, reduced endothelial nitric oxide production might be a principal factor in the increased aortic tone and, consequently, larger pulsatile energy in subjects with higher FFA. Insulin increases aortic tone by activating the sympathetic nervous system under the condition of insulin resistance. However, given the weak relationship between serum FFA and insulin levels, the involvement of insulin-mediated sympathetic activation might be independent of the effect of FFA. This is supported by the results of our regression analysis that show the insulin-independent association of FFA with baPWV.

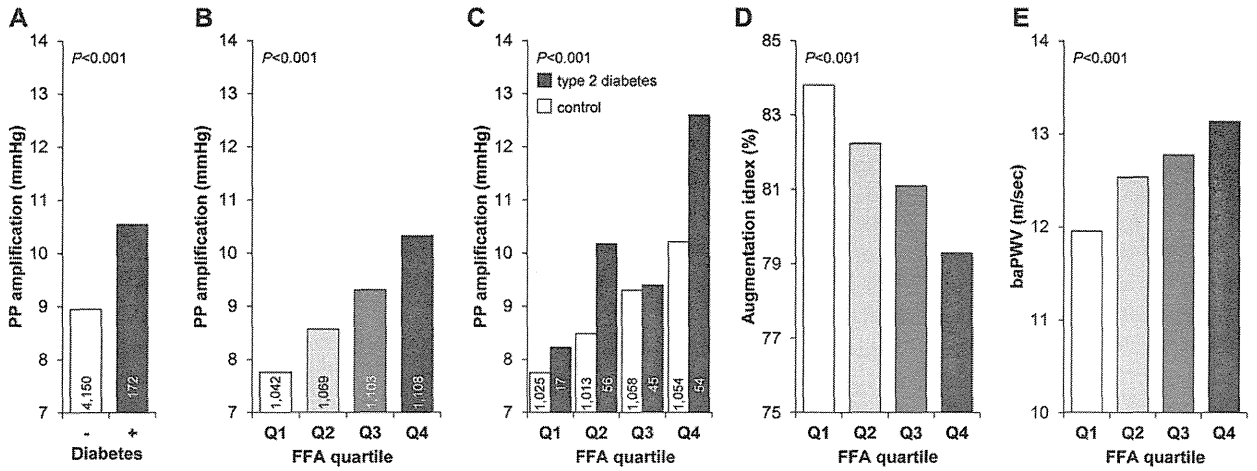

Figure 2. Association of free fatty acid (FFA) quartile with central hemodynamic parameters (study panel). Number of study participants in each subgroup are shown in the column. Statistical significance was assessed by analysis of variance. **A**, **B**, and **C**, pulse pressure (PP) amplification; **D**, augmentation index; **E**, brachia-to-ankle pulse wave velocity (baPWV).

We also investigated associations between plasma lipid parameters and PP amplification, but no remarkable relationships were observed after adjustment for basic covariates. These results further emphasize the importance of serum FFA, but not lipid profile, as a factor involved in central hemodynamics. A previous study in Australia[27] reported that obesity, particularly visceral adiposity, was significantly associated with smaller AIx. As serum FFA is mostly released from enlarged and stressed adipose tissue,[28] FFA might be a confounding factor in the inverse association between visceral adiposity and smaller AIx. No association between waist circumference and AIx was observed in the present study, which supports our hypothesis.

The maximum difference in PP amplification among all FFA quartiles was ≈2.5 mm Hg. This BP difference was somewhat larger than that observed in our previous reports of the association of smoking intensity[29] and insulin sensitivity.[12] The combination of FFA quartile and type 2 diabetes mellitus status further increased the maximum PP difference to 4.9 mm Hg. A previous clinical study, the Conduit Artery Function Evaluation (CAFE) study,[8] clearly indicated that even a 3-mm Hg difference between brachial and central SBP was associated with improved cardiovascular outcomes. Further, several studies have shown that an increase in central SBP of only 1 mm Hg has a substantial effect on large arterial remodeling[30] and silent cerebral damage.[31] Our findings therefore emphasize the importance of measuring serum FFA levels as a potential factor that modulates central hemodynamics and of measuring central BP in epidemiological and clinical settings.

Several limitations to the present study warrant mention. First, we did not directly measure transit time and magnitude of reflection pressure wave. As transit time largely correlate with baPWV, we deduced from results of the regression analysis that reduced magnitude rather than delayed arrival of reflection pressure wave might be involved in the paradoxical relationship between FFA and better central hemodynamic

Table 3. Multiple Linear Regression Analysis for Central Hemodynamic Parameters

Study Panel	Independent Variables	PP Amplification		AIx		Central SBP	baPWV
		Model 1	Model 2	Model 3	Model 4	Model 5	Model 6
Study panel (n=4322)	Type 2 diabetes mellitus	0.027 (0.039)	0.015 (0.007)	−0.014 (0.233)	−0.012 (0.315)	−0.008 (0.039)	0.061 (<0.001)
	Insulin (log-transformed)	0.003 (0.855)	0.019 (0.004)	0.023 (0.100)	0.016 (0.241)	−0.001 (0.855)	0.071 (<0.001)
	AIx, %		−1.004 (<0.001)				
	FFA, mEq/L	0.146 (<0.001)	0.022 (<0.001)		−0.123 (<0.001)	−0.044 (<0.001)	0.069 (<0.001)
Replication panel (n=5071)	Type 2 diabetes mellitus	0.038 (0.001)	0.020 (<0.001)	−0.016 (0.130)	−0.018 (0.082)	−0.012 (0.001)	0.055 (<0.001)
	Insulin (log-transformed)	0.028 (0.043)	0.037 (<0.001)	0.049 (<0.001)	0.009 (0.497)	−0.009 (0.043)	0.082 (<0.001)
	AIx (%)		−1.003 (<0.001)				
	FFA (mEq/L)	0.138 (<0.001)	0.023 (<0.001)		−0.115 (<0.001)	−0.045 (<0.001)	0.051 (<0.001)

Values are standardized regression coefficients (β). *P* values are shown in parenthesis. Adjusted factors were as follows: age, sex, body height, body weight, taking medication for hypertension or dyslipidemia, SBP, heart rate, total cholesterol, and baPWV. In regression Model 6, heart rate and baPWV were not adjusted. AIx indicates augmentation index; baPWV, brachial-to-ankle pulse wave velocity; FFA, free fatty acid; PP, pulse pressure; and SBP, systolic blood pressure.

profiles. More detailed waveform analysis would be needed to obtain conclusive evidence. Second, as this was a cross-sectional study, a longitudinal study is required to confirm the prognostic significance of central SBP differences arising from differences in serum FFA levels. Third, no information on the class of antihypertensive drugs was available for the Nagahama cohort sample, though β-blockers and vasodilators have substantial class effects on central BP that are well documented.[4–8] Given that the associations of FFA quartile with AIx and PPa were independent of antihypertensive medication, our results might be nondifferential and independent of the class effects of antihypertensive drugs.

Perspectives

In conclusion, we found that serum FFA level is an important factor influencing central hemodynamics. Our results might help identify the as yet unidentified mechanisms behind the favorable effects of insulin resistance and type 2 diabetes mellitus on the central hemodynamic profile.

Acknowledgments

We are extremely grateful to Drs Yoshihiko Kotoura, Miyaki Koichi and Ishizaki Tatsuro for their help in clinical measurements and the Nagahama City Office and nonprofit organization Zeroji Club for their help in conducting the Nagahama study. We thank the editors of Digital Medical Communications (DMC) Corporation for their help in the preparation of this article.

Sources of Funding

This study was supported by a University Grant and Grant-in-Aid for Scientific Research from the Ministry of Education, Culture, Sports, Science & Technology in Japan and a research grant from the Takeda Science Foundation.

Disclosures

The authors have no conflicts of interest to disclose.

References

1. Pini R, Cavallini MC, Palmieri V, Marchionni N, Di Bari M, Devereux RB, Masotti G, Roman MJ. Central but not brachial blood pressure predicts cardiovascular events in an unselected geriatric population: the ICARe Dicomano Study. *J Am Coll Cardiol*. 2008;51:2432–2439.
2. Roman MJ, Devereux RB, Kizer JR, Lee ET, Galloway JM, Ali T, Umans JG, Howard BV. Central pressure more strongly relates to vascular disease and outcome than does brachial pressure: the Strong Heart Study. *Hypertension*. 2007;50:197–203.
3. Vlachopoulos C, Aznaouridis K, O'Rourke MF, Safar ME, Baou K, Stefanadis C. Prediction of cardiovascular events and all-cause mortality with central haemodynamics: a systematic review and meta-analysis. *Eur Heart J*. 2010;31:1865–1871.
4. Williams B, Lacy PS, Thom SM, Cruickshank K, Stanton A, Collier D, Hughes AD, Thurston H, O'Rourke M; CAFE Investigators; Anglo-Scandinavian Cardiac Outcomes Trial Investigators; CAFE Steering Committee and Writing Committee. Differential impact of blood pressure-lowering drugs on central aortic pressure and clinical outcomes: principal results of the Conduit Artery Function Evaluation (CAFE) study. *Circulation*. 2006;113:1213–1225.
5. Boutouyrie P, Achouba A, Trunet P, Laurent S; EXPLOR Trialist Group. Amlodipine-valsartan combination decreases central systolic blood pressure more effectively than the amlodipine-atenolol combination: the EXPLOR study. *Hypertension*. 2010;55:1314–1322.
6. Ding FH, Li Y, Li LH, Wang JG. Impact of heart rate on central hemodynamics and stroke: a meta-analysis of β-blocker trials. *Am J Hypertens*. 2013;26:118–125.
7. Miyashita H, Aizawa A, Hashimoto J, Hirooka Y, Imai Y, Kawano Y, Kohara K, Sunagawa K, Suzuki H, Tabara Y, Takazawa K, Takenaka T, Yasuda H, Shimada K. Cross-sectional characterization of all classes of antihypertensives in terms of central blood pressure in Japanese hypertensive patients. *Am J Hypertens*. 2010;23:260–268.
8. Safar ME, Levy BI, Struijker-Boudier H. Current perspectives on arterial stiffness and pulse pressure in hypertension and cardiovascular diseases. *Circulation*. 2003;107:2864–2869.
9. Chirinos JA, Kips JG, Roman MJ, Medina-Lezama J, Li Y, Woodiwiss AJ, Norton GR, Yasmin, Van Bortel L, Wang JG, Cockcroft JR, Devereux RB, Wilkinson IB, Segers P, McEniery CM. Ethnic differences in arterial wave reflections and normative equations for augmentation index. *Hypertension*. 2011;57:1108–1116.
10. Agnoletti D, Lieber A, Zhang Y, Protogerou AD, Borghi C, Blacher J, Safar ME. Central hemodynamic modifications in diabetes mellitus. *Atherosclerosis*. 2013;230:315–321.
11. Tomita H, Kawamoto R, Tabara Y, Miki T, Kohara K. Blood pressure is the main determinant of the reflection wave in patients with type 2 diabetes. *Hypertens Res*. 2008;31:493–499.
12. Tabara Y, Saito I, Nishida W, Kohara K, Sakurai S, Kawamura R, Onuma H, Takata Y, Osawa H, Miki T, Tanigawa T. Relatively lower central aortic pressure in patients with impaired insulin sensitivity and resistance: the Toon Health Study. *J Hypertens*. 2011;29:1948–1954.
13. Chirinos JA, Segers P, Gillebert TC, De Buyzere ML, Van Daele CM, Khan ZA, Khawar U, De Bacquer D, Rietzschel ER; Asklepios Investigators. Central pulse pressure and its hemodynamic determinants in middle-aged adults with impaired fasting glucose and diabetes: the Asklepios study. *Diabetes Care*. 2013;36:2359–2365.
14. London GM, Pannier B. Arterial functions: how to interpret the complex physiology. *Nephrol Dial Transplant*. 2010;25:3815–3823.
15. Kim JA, Montagnani M, Koh KK, Quon MJ. Reciprocal relationships between insulin resistance and endothelial dysfunction: molecular and pathophysiological mechanisms. *Circulation*. 2006;113:1888–1904.
16. Boden G. Obesity, insulin resistance and free fatty acids. *Curr Opin Endocrinol Diabetes Obes*. 2011;18:139–143.
17. Takazawa K, Kobayashi H, Shindo N, Tanaka N, Yamashina A. Relationship between radial and central arterial pulse wave and evaluation of central aortic pressure using the radial arterial pulse wave. *Hypertens Res*. 2007;30:219–228.
18. Pauca AL, Kon ND, O'Rourke MF. The second peak of the radial artery pressure wave represents aortic systolic pressure in hypertensive and elderly patients. *Br J Anaesth*. 2004;92:651–657.
19. Kohara K, Tabara Y, Tomita H, Nagai T, Igase M, Miki T. Clinical usefulness of the second peak of radial systolic blood pressure for estimation of aortic systolic blood pressure. *J Hum Hypertens*. 2009;23:538–545.
20. Yamashina A, Tomiyama H, Takeda K, Tsuda H, Arai T, Hirose K, Koji Y, Hori S, Yamamoto Y. Validity, reproducibility, and clinical significance of noninvasive brachial-ankle pulse wave velocity measurement. *Hypertens Res*. 2002;25:359–364.
21. Tanaka H, Munakata M, Kawano Y, Ohishi M, Shoji T, Sugawara J, Tomiyama H, Yamashina A, Yasuda H, Sawayama T, Ozawa T. Comparison between carotid-femoral and brachial-ankle pulse wave velocity as measures of arterial stiffness. *J Hypertens*. 2009;27:2022–2027.
22. Lacy PS, O'Brien DG, Stanley AG, Dewar MM, Swales PP, Williams B. Increased pulse wave velocity is not associated with elevated augmentation index in patients with diabetes. *J Hypertens*. 2004;22:1937–1944.
23. Tamminen M, Westerbacka J, Vehkavaara S, Yki-Järvinen H. Insulin-induced decreases in aortic wave reflection and central systolic pressure are impaired in type 2 diabetes. *Diabetes Care*. 2002;25:2314–2319.
24. Westerbacka J, Wilkinson I, Cockcroft J, Utriainen T, Vehkavaara S, Yki-Järvinen H. Diminished wave reflection in the aorta. A novel physiological action of insulin on large blood vessels. *Hypertension*. 1999;33:1118–1122.
25. Odaira M, Tomiyama H, Hashimoto H, Kojima I, Matsumoto C, Yoshida M, Shiina K, Nagata M, Miyawaki Y, Yamashina A. Increased arterial stiffness weakens the relationship between wave reflection and the central pressure indexes in men younger than 60 years of age. *Am J Hypertens*. 2011;24:881–886.
26. Zhou W, Hong M, Zhang K, Chen D, Han W, Shen W, Zhu D, Gao P. Mechanisms of improved aortic stiffness by arotinolol in spontaneously hypertensive rats. *PLoS One*. 2014;9:e88722.
27. Maple-Brown LJ, Piers LS, O'Rourke MF, Celermajer DS, O'Dea K. Central obesity is associated with reduced peripheral wave reflection in Indigenous Australians irrespective of diabetes status. *J Hypertens*. 2005;23:1403–1407.

28. Boden G. Obesity, insulin resistance and free fatty acids. *Curr Opin Endocrinol Diabetes Obes*. 2011;18:139–143.
29. Tabara Y, Takahashi Y, Setoh K, Muro S, Kawaguchi T, Terao C, Kosugi S, Sekine A, Yamada R, Mishima M, Nakayama T, Matsuda F; Nagahama Study Group. Increased aortic wave reflection and smaller pulse pressure amplification in smokers and passive smokers confirmed by urinary cotinine levels: the Nagahama Study. *Int J Cardiol*. 2013;168:2673–2677.
30. Boutouyrie P, Bussy C, Lacolley P, Girerd X, Laloux B, Laurent S. Association between local pulse pressure, mean blood pressure, and large-artery remodeling. *Circulation*. 1999;100:1387–1393.
31. Shrestha I, Takahashi T, Nomura E, Ohtsuki T, Ohshita T, Ueno H, Kohriyama T, Matsumoto M. Association between central systolic blood pressure, white matter lesions in cerebral MRI and carotid atherosclerosis. *Hypertens Res*. 2009;32:869–874.

Novelty and Significance

What Is New?

- Elevated serum–free fatty acid (FFA) levels were strongly associated with reduced magnitude of arterial reflection pressure wave and relatively low central blood pressure.
- Central pressure differs by ≈4.9 mm Hg because of serum FFA levels and diabetic status.

What Is Relevant?

- Insulin resistance and diabetic status have been shown to be favorably associated with arterial waveform and central blood pressure.

Serum FFA was a more prominent determinant of arterial waveform than insulin.

Summary

Serum FFA was a factor that was favorably associated with central hemodynamics. A favorable association of FFA with central BP and arterial waveform suggests the importance of insulin signaling as a modulator of central hemodynamics.

Comprehensive Molecular Diagnosis of a Large Cohort of Japanese Retinitis Pigmentosa and Usher Syndrome Patients by Next-Generation Sequencing

Maho Oishi,[1] Akio Oishi,[1] Norimoto Gotoh,[2] Ken Ogino,[1] Koichiro Higasa,[2] Kei Iida,[3] Yukiko Makiyama,[1] Satoshi Morooka,[1] Fumihiko Matsuda,[2] and Nagahisa Yoshimura[1]

[1]Department of Ophthalmology and Visual Sciences, Kyoto University Graduate School of Medicine, Kyoto, Japan
[2]Center for Genomic Medicine, Kyoto University Graduate School of Medicine, Kyoto, Japan
[3]Medical Research Support Center, Kyoto University Graduate School of Medicine, Kyoto, Japan

Correspondence: Akio Oishi, 54 Kawahara, Shogoin, Sakyo, Kyoto 606-8507, Japan; aquio@kuhp.kyoto-u.ac.jp.

Submitted: August 13, 2014
Accepted: October 7, 2014

Citation: Oishi M, Oishi A, Gotoh N, et al. Comprehensive molecular diagnosis of a large cohort of Japanese retinitis pigmentosa and Usher syndrome patients by next-generation sequencing. *Invest Ophthalmol Vis Sci.* 2014;55:7369–7375. DOI: 10.1167/iovs.14-15458

Purpose. Retinitis pigmentosa (RP), a major cause of blindness in developed countries, has multiple causative genes; its prevalence differs by ethnicity. Usher syndrome is the most common form of syndromic RP and is accompanied by hearing impairment. Although molecular diagnosis is challenging, recent technological advances such as targeted high-throughput resequencing are efficient screening tools.

Methods. We performed comprehensive molecular testing in 329 Japanese RP and Usher syndrome patients by using a custom capture panel that covered the coding exons and exon/intron boundaries of all 193 known inherited eye disease genes combined with Illumina HiSequation 2500. Candidate variants were screened using systematic data analyses, and their potential pathogenicity was assessed according to the frequency of the variants in normal populations, in silico prediction tools, and compatibility with known phenotypes or inheritance patterns.

Results. Molecular diagnoses were made in 115/317 RP patients (36.3%) and 6/12 Usher syndrome patients (50%). We identified 104 distinct mutations, including 66 novel mutations. *EYS*, *USH2A*, and *RHO* were common causative genes. In particular, mutations in *EYS* accounted for 15.0% of the autosomal recessive/simplex RP patients or 10.7% of the entire RP cohort. Among the 189 previously reported mutations detected in the current study, 55 (29.1%) were found commonly in Japanese or other public databases and were excluded from molecular diagnoses.

Conclusions. By screening a large cohort of patients, this study catalogued the genetic variations involved in RP and Usher syndrome in a Japanese population and highlighted the different distribution of causative genes among populations.

Keywords: retinitis pigmentosa, Usher syndrome, next-generation sequencing, targeted resequencing

Retinitis pigmentosa (RP) is the most frequent subtype of inherited retinal degeneration, and its prevalence is 1 in 3000 to 5000 individuals worldwide.[1] Retinitis pigmentosa is clinically and genetically heterogeneous. For example, RP accompanied by hearing impairment is termed Usher syndrome, which is the most common form of syndromic RP. To date, mutations in 73 genes are known to be responsible for RP or Usher syndrome. In addition, 141 genes are associated with other subtypes of inherited retinal diseases (RetNet, https://sph.uth.edu/retnet/ [in the public domain]). However, no known single gene mutation accounts for more than 10% of RP patients in any reported studies.[2] Although the screening of known genes should be the first step for identifying novel causative genes, sequencing all these genes in individual patients has been virtually impossible.

In principle, the causative gene cannot be predicted from the phenotype. Inheritance patterns, which include autosomal dominant (ad), autosomal recessive (ar), X-linked (xl), digenic,[3] and maternal or mitochondrial,[4,5] can help to narrow down the number of candidate genes. However, the inheritance pattern cannot always be determined because of patients' insufficient memory or lack of information regarding their family history. In addition, mutations in the same gene sometimes cause different phenotypes or different inheritance traits, which make examinations complicated.

The most widely used methods for the molecular diagnosis of RP, such as Sanger sequencing and arrayed primer extension (APEX) chips (Asper Ophthalmics, Tartu, Estonia), have limitations. The Sanger technique can determine sequences accurately; however, it is labor-intensive, time-consuming, and cost-prohibitive for screening multiple genes. Arrayed primer extension is designed to detect only selected known mutations; therefore, a novel mutation cannot be detected. Specifically, the detection rate of APEX is <10% to 15%,[6] or even lower, depending on the ethnicity of the patients.[7]

Recently, the development of next-generation sequencing (NGS) technology enabled the sequencing of all exons or even the whole genome of an individual. The technology had been

applied to RP/Usher syndrome, and several studies reported a significantly higher diagnosis rate (25%–55%) compared with that achieved using conventional methods.[8–14] Furthermore, the results revealed a different prevalence of causative genes among different ethnicities. For example, studies conducted in North America or China did not report patients with mutations in *EYS*,[11,12] which comprise ~20% of arRP cases in Japan,[15,16] or with mutations in *DHDDS*, which account for ~10% of arRP cases in Ashkenazi Jewish populations.[17,18] These results highlight the importance of making specific genetic catalogues for each ethnicity.

In the current study, we performed a comprehensive molecular analysis of 329 Japanese RP or Usher syndrome patients. We analyzed all retinal and optic nerve disease genes reported in the RetNet database at the time of designing this study (193 genes). In addition, in an attempt to identify novel causative genes, an additional 172 genes were also analyzed using a custom-designed targeted resequencing technique.

Methods

All procedures used in this study adhered to the tenets of the Declaration of Helsinki. The institutional review boards and the ethics committees of each institution approved the study protocols. All patients and their relatives were fully informed of the purpose and procedures of this study, and written consent was obtained from each participant.

Study Subjects

We examined 329 Japanese patients with RP who visited the Department of Ophthalmology and Visual Sciences, Kyoto University Graduate School of Medicine, Kyoto, Japan, between January 2011 and December 2012 and agreed to participate in the study. Among these, 12 patients exhibited hearing impairment and were diagnosed with Usher syndrome. An additional 26 cases with various forms of inherited retinal diseases, carrying known variants, were investigated to evaluate the integrity of the current approach.

Retina specialists made all diagnoses of RP based on comprehensive ophthalmologic examinations, and disorder of hearing and/or equilibrium was confirmed by otolaryngologists in Usher syndrome cases. All patients underwent visual acuity measurements, slit-lamp biomicroscopy, ophthalmoscopy, fundus photography, optical coherence tomography, Goldman visual field testing, and electroretinography, according to the protocol of the International Society for Clinical Electrophysiology of Vision.[19] Wide-field fundus autofluorescence[20] was also available for most patients. Pedigrees were constructed based on patient interviews. A peripheral blood sample was taken from every patient and his or her family members when available. Genomic DNA was extracted from the peripheral blood by using a DNA extraction kit (QuickGene-610L; Fujifilm, Minato, Tokyo, Japan). The quantity and quality of the DNA were verified using a dsDNA HS Assay kit on a Qubit (Life Technologies, Carlsbad, CA, USA) and a NanoDrop spectrophotometer (Thermo Scientific, Waltham, MA, USA).

Target Capture and Next-Generation Sequencing

Target regions were captured using reagents from a custom-design HaloPlex Target Enrichment kit 2.5 Mb (Agilent Technologies, Santa Clara, CA, USA), according to the HaloPlex Target Enrichment System Automation Protocol for Illumina Sequencing Version D.2. SureDesign software (Agilent Technologies) was used to design the custom HaloPlex capture assay. The capture panel consisted of 2,433,298 base pairs (bp) covering all coding and noncoding exons with flanking exon/intron boundaries (±25 bp) of 365 genes, including all 193 retinal and optical disease genes that had been reported in RetNet at the time of designing this study (December 26, 2012), as well as the 172 genes expressed at the highest level in rod or cone photoreceptors (Supplementary Table S1).[21] Precapture Illumina libraries were then generated according to the manufacturer's protocol. Briefly, the protocol consisted of the following four steps: (1) digestion of 225 ng genomic DNA in eight different restriction reactions; (2) hybridization of the digested fragments to probes whose ends are complementary to the target fragments (during hybridization, the fragments were circularized and sequencing motifs, including index sequences, were incorporated); (3) capture of the target DNA using streptavidin beads followed by ligation of the circularized fragments; (4) PCR amplification of the captured target libraries, followed by purification and adaptor-dimer removal by using AMPure XP beads (Beckman Coulter, Brea, CA, USA). For each capture reaction, 47 or 48 libraries were pooled. The concentration of the pooled libraries was determined using a 2100 Bioanalyzer (Agilent Technologies). The pooled libraries were quantified and sequenced on the Illumina HiSequation 2500 as 100-bp paired-end reads following the manufacturer's protocols.

Data Analysis

Sequence reads were aligned to the reference genome (National Center for Biotechnology Information [NCBI] Build 37) by using the Burrows-Wheeler Aligner[22] after trimming the adapter sequence (AGATCG) using custom Perl script. After recalibration of base quality values and local realignment, single nucleotide variant and insertion/deletion (indel) calling was performed using the Genome Analysis Toolkit.[23] To filter out common SNPs and indels, dbSNP (Build 138) (NCBI, http://www.ncbi.nlm.nih.gov/SNP/ [in the public domain]), 1000 Genomes,[24] National Heart, Lung and Blood Institute GO Exome Sequencing Project (ESP6500, http://evs.gs.washington.edu/EVS/ [in the public domain]), and the Human Genetic Variation Database (HGVD; http://www.genome.med.kyoto-u.ac.jp/SnpDB/ [in the public domain]) databases were used. The HGVD contains genetic variations determined using the exome sequencing of 1208 Japanese control subjects. Variant annotation was performed using ANNOVAR.[25] To assess the pathogenicity of novel missense variants, five types of prediction scores for amino acid substitutions (SIFT, Polyphen2, LRT, MutationTaster, and MutationAssessor) and two conservation scores (PhyloP and GERP++) obtained from dbNSFP[26] were used.

Interpretation of the Genetic Variants

Several criteria were applied to select variants for further analysis and to filter out putative false positives caused by alignment artifacts. Analysis focused on variants of the 193 genes reported in RetNet database, which includes all known retinal disease genes. First, variants were selected within coding exons or intronic variants ±25 bp from the exon boundaries. Second, variants that covered <10× were excluded. Third, synonymous variants and nonframeshift indels were excluded unless they were listed in the Human Gene Mutation Database (HGMD; BIOBASE, Wolfenbüttel, Lower Saxony, Germany) or were reported previously as being pathogenic alterations. However, it should be noted that this step might filter out true pathogenic variants.

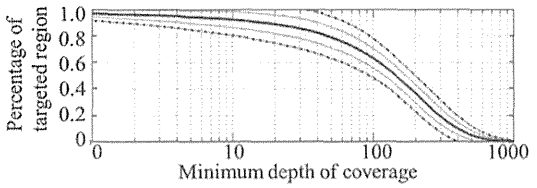

FIGURE 1. The percentage of the targeted regions (*y*-axis) that achieved a certain minimum coverage (*x*-axis). The *solid curve* represents the mean of 329 samples, whereas the *dotted* and *dashed lines* indicate one and two standard deviations, respectively. The data reveal that 92.2% of the targeted regions are covered by >10×.

Determination of the Pathogenicity of the Variants

A variant was classified as pathogenic if the following criteria applied. (1) Because RP is a rare Mendelian disease, variants were excluded that had an allele frequency > 0.5% (for recessive variants) or >0.1% (for dominant variants) in any of the 1000 Genomes database, ESP6500 database, or HGVD. (2) Mutations listed in the HGMD or those identified as pathogenic alterations in previous publications were regarded as pathogenic. (3) Nonsense and frameshift variants were also considered as pathogenic. (4) For a novel missense variant, in silico prediction programs were used to predict its pathogenicity. Only novel missense variants that were predicted to be pathogenic by at least five of seven well-established algorithms were reported. Variants that were predicted to be pathogenic by at least three of five missense prediction programs (SIFT, Polyphen2, LRT, MutationTaster, and MutationAssessor) and whose evolutionary conservation scores were >0 in both PhyloP and GERP++ were considered to be pathogenic. (5) For splice-site variants, the prediction program MaxEntScan was used, and these were considered pathogenic if the score differed by >5 between the wild-type and mutated sequences.[27] (6) Variants were adopted that matched the patients' phenotype and the reported inheritance pattern of the respective genes.

Pathogenic variants in the dominant genes found in simplex cases were regarded as disease-causing mutations only when they were published previously or were confirmed to be a de novo mutation by using parental testing. Variants with a frequency more than that mentioned in criterion 1 were excluded even if they were listed in the HGMD or in previously published reports. All mutations and potential pathogenic variants detected using NGS were validated using conventional Sanger sequencing. Sequencing was performed using an Applied Biosystems (ABI) 3130xl Genetic Analyzer (Life Technologies). Segregation analysis was performed if DNA from family members was available.

Evaluation of the Sensitivity of the Method

Twenty-six cases carrying 33 known variants in various genes were included as positive controls to evaluate the integrity of the current approach (Supplementary Table S2). All variants were detected using the APEX chip and confirmed using Sanger sequencing before the current study was conducted.

Results

A total of 329 patients, including 77 adRP, 73 arRP, 6 xlRP, 161 simplex RP, and 12 Usher syndrome patients, were studied. Among these, two pairs of adRP cases and one pair of arRP cases had a blood relationship (two pairs of adRP cases had a parent-child relationship, whereas one pair of arRP cases comprised siblings).

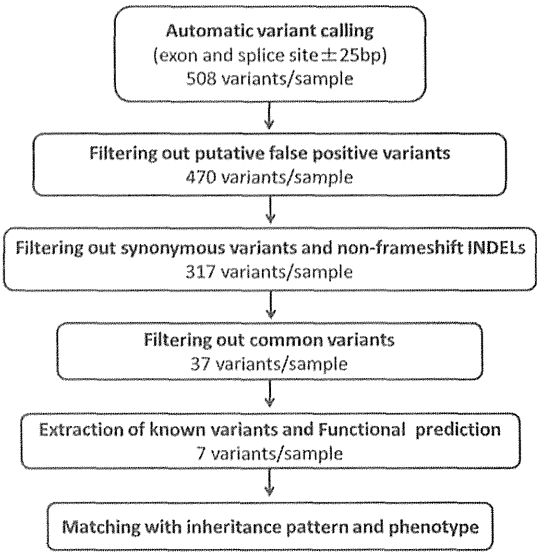

FIGURE 2. The data analysis pipeline used to filter and identify the putative pathogenic mutations in this study. Three public databases and seven in silico programs were used to evaluate the pathogenicity of variants. This stringent filtering should have excluded false-positive variants.

Targeted Sequencing and Data Processing

All exons and the regions 25 bp upstream and downstream of 365 genes were enriched using targeted capture and sequenced using NGS. For each sample, a mean of 7,548,920 reads was generated, approximately 82.2% of which were mapped to the targeted regions. Although a small number of samples (74/329, 22.5%) had relatively low coverage compared with the others (Supplementary Fig. S1), the mean and median coverage of the 193 RetNet genes in all samples was 250× and 242×, respectively. Within the targeted region, 92.2% of the bases had coverage > 10×, and 88.7% of the bases had coverage > 20×, suggesting that sufficient coverage was achieved (Fig. 1). Among the 3619 targeted exons, only 1.58% covered < 5× (Supplementary Table S3).

For each sample, a mean of 1577 raw variants and small indels were identified initially by using automated variant detection. After filtering out putative false-positive variants and synonymous or nonframeshift variants, a mean of 317 variants remained. After excluding common variants in any of the variant databases (as described in Materials and Methods section on interpretation of genetic variants), functional prediction tools were applied, and a mean 7.08 rare variants that were likely to cause a deleterious protein coding change were detected per sample (Fig. 2).

Identification of Mutations in Positive Controls

All 33 variants present in the 26 positive control samples were detected, in spite of stringent filtering steps taken to exclude putative false-positive variants. This indicates that the combination of HaloPlex and Illumina HiSeq resulted in high-sensitivity sequencing and confirmed validity of the data processing methods (Supplementary Table S2).

Identification of Pathogenic Mutations in 329 RP or Usher Syndrome Patients

Mutations listed in the HGMD or in previous publications as causing retinal diseases, as well as novel pathogenic variants

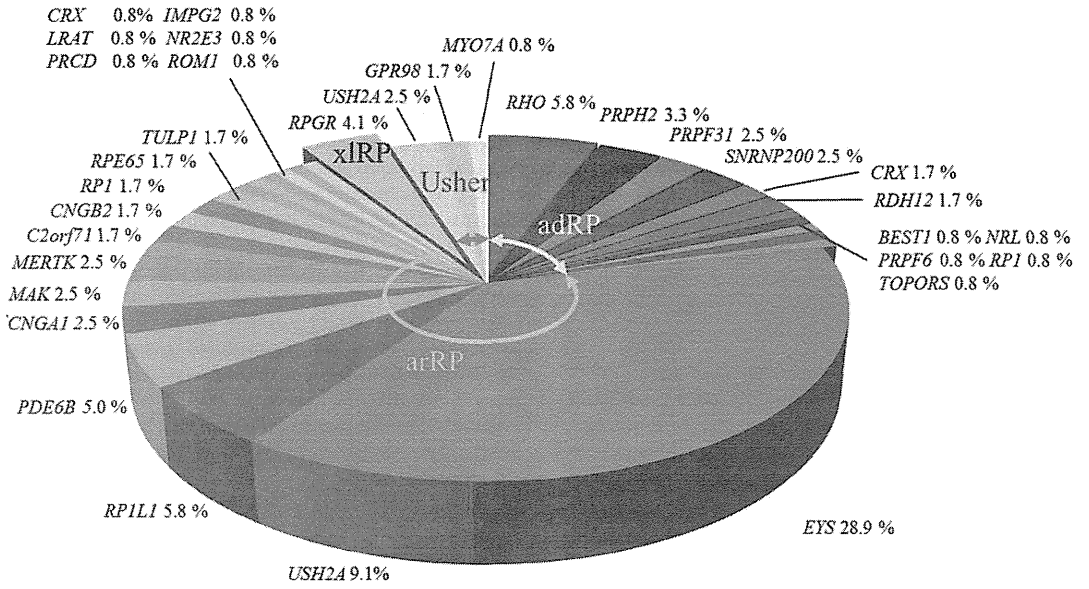

FIGURE 3. The percentage of causative genes with each inheritance trait that were identified in 115 RP patients and six Usher syndrome patients. Mutations in *EYS* and *USH2A* were common in the population.

that were predicted to be pathogenic after the stringent filtering steps, were identified. Specifically, pathogenic mutations were identified for 115/317 (36.3%) RP patients and 6/12 (50%) Usher syndrome patients. A total of 103 distinct mutations were identified, including a large number of novel mutations (n = 65). The novel mutations consisted of 23 missense (35.4%), 19 frameshift (29.2%), 17 nonsense (26.2%), and six splice-site (9.2%) mutations (Supplementary Tables S4-S9). The pathogenicity of the novel missense mutations was supported by a combination of in silico prediction programs (Supplementary Table S8). A summary of the causative genes is shown in Figure 3 and the Table.

Patients Carrying Mutations in Known RP Genes. We identified 121 patients who carried pathogenic mutations in known RP or Usher syndrome genes (Supplementary Tables S4-S6). The diagnostic efficiency of each hereditary form was 27/77 (35.1%) in adRP, 37/73 (50.7%) in arRP, 1/6 (16.7%) in xlRP, 50/161 (31.1%) in simplex RP, and 6/12 (50%) in Usher syndrome. Among the 50 simplex cases whose mutations were identified, 3 were due to mutations in ad genes (K6413, K6210, and K6419). One of the 77 ad cases and 3 of 161 simplex cases turned out to be xl with mutations in *RPGR* (K1881, K6101, K6170, and K6292). Three cases initially diagnosed as ad were determined to be ar with known mutations in *EYS* (K6006, K6105, and K6195).

We identified 48 patients carrying mutations that are known to cause RP or Usher syndrome (Supplementary Table S4). Among these cases diagnosed with high confidence, 24/48 (50.0%) patients carried mutations in the *EYS* gene. Proband K1908 and proband K6184 had three mutations, including a novel nonsense mutation c.1750G>T in *EYS* or a novel missense mutation c.2653C>T in *USH2A*, respectively.

Forty-five patients carried at least one novel loss-of-function (LOF) mutation (nonsense, frameshift, or splicing mutations) in known RP or Usher syndrome genes (Supplementary Table S5). Among this group diagnosed with relatively high confidence, 44 distinct pathogenic mutations were identified, including 6 previously reported mutations. One pair of familial cases (K6001 and K6003) was included in this group.

In addition, 28 patients who carried one or more novel putative missense mutations in RP or Usher syndrome genes

TABLE. List of the Causative Genes in 121 RP and Usher Syndrome Patients Identified in the Current Study

Gene	n
RP	
EYS	35
USH2A	11
RHO	7
RP1L1	7
PDE6B	6
RPGR	5
PRPH2	4
CNGA1	3
CRX	3
MAK	3
MERTK	3
PRPF31	3
RP1	3
SNRNP200	3
C2orf71	2
CNGB1	2
RDH12	2
RPE65	2
TULP1	2
BEST1	1
IMPG2	1
LRAT	1
NR2E3	1
NRL	1
PRCD	1
PRPF6	1
ROM1	1
TOPORS	1
Usher syndrome	
USHA2A	3
GPR98	2
MYO7A	1
Total	121

were identified (Supplementary Table S6). In this group with lower confidence diagnosis, 32 distinct pathogenic mutations were identified, including 3 previously reported mutations, 3 novel LOF mutations, and 26 novel missense mutations in 17 genes.

Patients Carrying Known Mutations in Other Retinal Disease Genes. Two patients carried reported mutations that are known to cause other retinal diseases (Supplementary Table S7). Proband K6043 carried c.1511A>G in *JAG1*, which causes Alagille syndrome. Proband K1956 carried c.808C>T in *CHM*, which causes choroideraemia.

Revision of the Initial Clinical Diagnosis

The clinical symptoms of all patients identified as carrying known mutations in other retinal diseases were carefully reassessed. In the group with lower confidence diagnoses, three patients (K6266, K6274, and K6348) carried mutations known to cause Best macular dystrophy, pattern dystrophy, or retinitis punctata albescens, respectively (Supplementary Table S6). Although these mutations have been reported to cause other retinal diseases, their clinical characteristics were typical of RP; therefore, these variants were classified as novel missense mutations that cause RP. All of these were variants in known RP genes, and their pathogenicity was supported by in silico prediction tools (Supplementary Table S8). In an additional two patients carrying known mutations in other retinal disease genes (Supplementary Table S7), the clinical diagnosis of xl case K1956, who carried a reported hemizygous nonsense mutation known to cause choroideraemia, was revised to choroideraemia. Choroideraemia is a nonsyndromic choroidal and retinal disease that presents with symptoms and clinical features similar to those of advanced RP. In contrast, the simplex case K6043, who carries a mutation known to cause Alagille syndrome, remains unsolved because of the lack of characteristic systemic disorders.

Reported Mutations With a High Allele Frequency in Public Databases

Using filtering and annotation procedures, some of the reported mutations were revealed to be common in healthy individuals. Because RP is a rare Mendelian disease, we considered that variants that had an allele frequency > 0.5% (for recessive variants) or >0.1% (for dominant variants) in any of the public databases were pathogenic in the current study. After these analyses, 55 of the 189 reported mutations known to cause retinal or optic nerve diseases were excluded (Supplementary Table S10).

Discussion

In the present study, we screened 329 Japanese RP or Usher syndrome patients, and made molecular diagnoses in 122 cases (37.1%). To our knowledge, the present cohort is the largest among those in studies using NGS for the comprehensive molecular diagnosis of RP. In addition, this was the first such study in Japanese individuals; the data confirmed the high prevalence of mutations in *EYS* and *USH2A* gene among this population.

The present study revealed that the prevalence of causative genes differed in Japanese populations compared with that in other ethnicities. The frequency of *EYS* mutations was up to 11% (35/317) in the Japanese RP population, which is the highest percentage by which a single gene accounts for RP.[2] The association between *EYS* mutations and RP was first reported in 2008.[28] Subsequently, several reports revealed a prevalence of *EYS* mutations of 5% to 10% of European arRP patients,[13,29,30] whereas the prevalence of *EYS*-associated RP was as high as 20% in Japanese arRP patients.[15,16] The present study confirmed the significant influence of *EYS* in Japanese populations. Specifically, the allele frequency of c.8805C>A and c.4957dupA, the most frequent mutations in *EYS*, in the control Japanese population was 0.34% and 0.32%, respectively. This high frequency of carriers accounts for the detection of *EYS* mutations in three probands who were presumed to be adRP.

The present results have some implications regarding a role for the *RP1L1* gene in RP. Homozygous mutations in *RP1L1* were found in seven patients, which account for 7.8% of the arRP cases. Although mutations in this gene were first reported in patients with ad occult macular dystrophy,[31] homozygous mutations of *RP1L1* were reported subsequently in patients with arRP.[32] The prevalence of *RP1L1* mutations in the current study was considerably higher than that reported in the previous study; Davidson et al.[32] revealed one patient by using homozygosity mapping, and only one other patient among 285 RP patients. Differences in the mutation allele frequency among ethnicities might also be observed in *RP1L1*. Because RP1L1 interacts with RP1, modifications to *RP1*-associated RP were also suggested.[33] However, none of the patients with putative disease-causing mutations in *RP1L1* carried mutations in *RP1* gene in the current study or in a previous report.[32] Therefore, the hypothesis that *RP1* and *RP1L1* cause digenic RP is yet to be confirmed.

Before the advent of NGS, screening using denaturing high-performance liquid chromatography (dHPLC) or high-resolution melting analysis followed by Sanger sequence was used to detect causative mutations in genetically heterogeneous diseases such as RP. Jin et al.[34] applied dHPLC and Sanger sequencing to Japanese RP patients and detected causative mutations in 14.1% of cases. The difference in the prevalence of causative mutations among ethnicities could partially explain the unsatisfactory detection rate in this previous report. The current study revealed the highest detection rate in Japanese populations to date, which was comparable to that in populations of other ethnicities.[8–14] These results confirm that comprehensive screening using NGS is an effective strategy, independent of the patient cohort.

The present results suggest that some of the previously reported mutations were not disease causing. In the present study, we used a public genome database containing 1208 healthy Japanese individuals, as well as the 1000 Genomes and ESP6500 databases to screen the candidate variants. This revealed that some mutations registered in the HGMD are common in Japanese populations, suggesting that these mutations were benign variants. Therefore, information regarding disease-causing mutations should be revised based on the current evidence.

We employed targeted exome resequencing rather than whole-exome sequencing (WES). Although WES could become a standard screening method in the near future, targeted exome resequencing retains some advantages. Specifically, it can achieve a higher coverage rate in the region of interest, and can screen more patients in a single assay, thereby lowering cost.[35] As such, targeted exome resequencing is a reasonable option to screen highly heterogeneous groups of diseases such as RP.

Although molecular diagnoses were made in 37.7% of the cases in the current study, causative mutations are yet to be elucidated in the remaining 62.3% of the patients. The technical and methodological limitations of our approach might be one of the reasons for this. We confirmed the sensitivity of the method using 26 patients carrying 33 variants identified previously.[7] Next-generation sequencing detected all

these variants successfully, which verified the high sensitivity of the current approach. However, NGS technology is not good at reading certain specific sequences including GC-rich regions, repeated sequences, copy-number variations, and large deletions. Intronic mutations, synonymous mutations, and nonframeshift mutations were also not covered by the current method. In addition, some cases resulted in relatively low coverage compared with the other samples. This might have been caused by technical challenges during the generation of precapture libraries. Although the mean coverage achieved was 244×, which seemed to be sufficient for the identification of variants, the percentage of bases covered >10× was 81%, and variants with low coverage were excluded (Supplementary Fig. S1). A more important reason for the lack of detection is insufficient knowledge of RP-causative genes. Although more than 60 causative genes have been identified to date, this number is still increasing. Therefore, further exploration of novel genes is required to achieve an optimal detection rate.

In conclusion, the present study screened the largest sample of Japanese RP patients to date and described the genetic catalogue for the cohort. The data confirmed differences in the RP-causative genes among ethnicities, and highlighted the importance of integrating studies from multiple populations for a deeper understanding of the disease-causing mutations. We are currently identifying novel genes in the captured candidates. Future studies including WES or even whole-genome sequencing in various ethnicities might boost the identification of novel causative genes of RP.

Acknowledgments

We thank Jun Zhu, PhD; Yoshiyuki Wakabayashi, PhD; and Yanqin Yang, MD, MSc, at DNA Sequencing and Computational Biology Core, National Heart, Lung and Blood Institute, National Institutes of Health, for their advice on technical issues and invaluable comments to improve the manuscript. DNA sequencing analysis with the Sanger method was performed at the Medical Research Support Center, Graduate School of Medicine, Kyoto University (chief director, Masatoshi Hagiwara, MD, PhD). We thank Hatsue Hamanaka for her technical support in the preparation and sequencing of the genetic samples.

Supported in part by the Japan Ministry of Health, Labour and Welfare (No. 12103069), a grant-in-aid for scientific research (No. 26861445), and the Japanese Retinitis Pigmentosa Society. The authors alone are responsible for the content and writing of the paper.

Disclosure: **M. Oishi**, None; **A. Oishi**, None; **N. Gotoh**, None; **K. Ogino**, None; **K. Higasa**, None; **K. Iida**, None; **Y. Makiyama**, None; **S. Morooka**, None; **F. Matsuda**, None; **N. Yoshimura**, None

References

1. Chizzolini M, Galan A, Milan E, Sebastiani A, Costagliola C, Parmeggiani F. Good epidemiologic practice in retinitis pigmentosa: from phenotyping to biobanking. *Curr Genomics*. 2011;12:260–266.
2. Wang DY, Chan WM, Tam PO, et al. Gene mutations in retinitis pigmentosa and their clinical implications. *Clin Chim Acta*. 2005;351:5–16.
3. Kajiwara K, Berson EL, Dryja TP. Digenic retinitis pigmentosa due to mutations at the unlinked peripherin/RDS and ROM1 loci. *Science*. 1994;264:1604–1608.
4. Lestienne P, Ponsot G. Kearns-Sayre syndrome with muscle mitochondrial DNA deletion. *Lancet*. 1988;1:885.
5. Moraes CT, DiMauro S, Zeviani M, et al. Mitochondrial DNA deletions in progressive external ophthalmoplegia and Kearns-Sayre syndrome. *N Engl J Med*. 1989;320:1293–1299.
6. Avila-Fernandez A, Cantalapiedra D, Aller E, et al. Mutation analysis of 272 Spanish families affected by autosomal recessive retinitis pigmentosa using a genotyping microarray. *Mol Vis*. 2010;16:2550–2558.
7. Ogino K, Oishi A, Makiyama Y, et al. Genotype screening of retinal dystrophies in the Japanese population using a microarray [in Japanese]. *Nihon Ganka Gakkai Zasshi*. 2013;117:12–18.
8. Simpson DA, Clark GR, Alexander S, Silvestri G, Willoughby CE. Molecular diagnosis for heterogeneous genetic diseases with targeted high-throughput DNA sequencing applied to retinitis pigmentosa. *J Med Genet*. 2011;48:145–151.
9. Neveling K, Collin RW, Gilissen C, et al. Next-generation genetic testing for retinitis pigmentosa. *Hum Mutat*. 2012;33:963–972.
10. Shanks ME, Downes SM, Copley RR, et al. Next-generation sequencing (NGS) as a diagnostic tool for retinal degeneration reveals a much higher detection rate in early-onset disease. *Eur J Hum Genet*. 2013;21:274–280.
11. Fu Q, Wang F, Wang H, et al. Next-generation sequencing-based molecular diagnosis of a Chinese patient cohort with autosomal recessive retinitis pigmentosa. *Invest Ophthalmol Vis Sci*. 2013;54:4158–4166.
12. Wang F, Wang H, Tuan HF, et al. Next generation sequencing-based molecular diagnosis of retinitis pigmentosa: identification of a novel genotype-phenotype correlation and clinical refinements. *Hum Genet*. 2014;133:331–345.
13. Glockle N, Kohl S, Mohr J, et al. Panel-based next generation sequencing as a reliable and efficient technique to detect mutations in unselected patients with retinal dystrophies. *Eur J Hum Genet*. 2014;22:99–104.
14. Xu Y, Guan L, Shen T, et al. Mutations of 60 known causative genes in 157 families with retinitis pigmentosa based on exome sequencing. *Hum Genet*. 2014;133:1255–1271.
15. Hosono K, Ishigami C, Takahashi M, et al. Two novel mutations in the EYS gene are possible major causes of autosomal recessive retinitis pigmentosa in the Japanese population. *PLoS One*. 2012;7:e31036.
16. Iwanami M, Oshikawa M, Nishida T, Nakadomari S, Kato S. High prevalence of mutations in the EYS gene in Japanese patients with autosomal recessive retinitis pigmentosa. *Invest Ophthalmol Vis Sci*. 2012;53:1033–1040.
17. Zelinger L, Banin E, Obolensky A, et al. A missense mutation in DHDDS, encoding dehydrodolichyl diphosphate synthase, is associated with autosomal-recessive retinitis pigmentosa in Ashkenazi Jews. *Am J Hum Genet*. 2011;88:207–215.
18. Zuchner S, Dallman J, Wen R, et al. Whole-exome sequencing links a variant in DHDDS to retinitis pigmentosa. *Am J Hum Genet*. 2011;88:201–206.
19. Marmor MF, Fulton AB, Holder GE, Miyake Y, Brigell M, Bach M. ISCEV standard for full-field clinical electroretinography (2008 update). *Doc Ophthalmol*. 2009;118:69–77.
20. Oishi A, Ogino K, Makiyama Y, Nakagawa S, Kurimoto M, Yoshimura N. Wide-field fundus autofluorescence imaging of retinitis pigmentosa. *Ophthalmology*. 2013;120:1827–1834.
21. Brooks MJ, Rajasimha HK, Roger JE, Swaroop A. Next-generation sequencing facilitates quantitative analysis of wild-type and Nrl(-/-) retinal transcriptomes. *Mol Vis*. 2011;17:3034–3054.
22. Li H, Durbin R. Fast and accurate short read alignment with Burrows-Wheeler transform. *Bioinformatics*. 2009;25:1754–1760.

23. DePristo MA, Banks E, Poplin R, et al. A framework for variation discovery and genotyping using next-generation DNA sequencing data. *Nat Genet.* 2011;43:491–498.
24. Abecasis GR, Altshuler D, Auton A, et al. A map of human genome variation from population-scale sequencing. *Nature.* 2010;467:1061–1073.
25. Wang K, Li M, Hakonarson H. ANNOVAR: functional annotation of genetic variants from high-throughput sequencing data. *Nucleic Acids Res.* 2010;38:e164.
26. Liu X, Jian X, Boerwinkle E. dbNSFP v2.0: a database of human non-synonymous SNVs and their functional predictions and annotations. *Hum Mutat.* 2013;34:E2393–E2402.
27. Yeo G, Burge CB. Maximum entropy modeling of short sequence motifs with applications to RNA splicing signals. *J Comput Biol.* 2004;11:377–394.
28. Abd El-Aziz MM, Barragan I, O'Driscoll CA, et al. EYS, encoding an ortholog of Drosophila spacemaker, is mutated in autosomal recessive retinitis pigmentosa. *Nat Genet.* 2008; 40:1285–1287.
29. Audo I, Sahel J-A, Mohand-Saïd S, et al. EYS is a major gene for rod-cone dystrophies in France. *Hum Mutat.* 2010;31:E1406–E1435.
30. Littink KW, van den Born LI, Koenekoop RK, et al. Mutations in the EYS gene account for approximately 5% of autosomal recessive retinitis pigmentosa and cause a fairly homogeneous phenotype. *Ophthalmology.* 2010;117:2026–2033, 2033 e1–7.
31. Akahori M, Tsunoda K, Miyake Y, et al. Dominant mutations in RP1L1 are responsible for occult macular dystrophy. *Am J Hum Genet.* 2010;87:424–429.
32. Davidson AE, Sergouniotis PI, Mackay DS, et al. RP1L1 variants are associated with a spectrum of inherited retinal diseases including retinitis pigmentosa and occult macular dystrophy. *Hum Mutat.* 2013;34:506–514.
33. Yamashita T, Liu J, Gao J, et al. Essential and synergistic roles of RP1 and RP1L1 in rod photoreceptor axoneme and retinitis pigmentosa. *J Neurosci.* 2009;29:9748–9760.
34. Jin ZB, Mandai M, Yokota T, et al. Identifying pathogenic genetic background of simplex or multiplex retinitis pigmentosa patients: a large scale mutation screening study. *J Med Genet.* 2008;45:465–472.
35. Sikkema-Raddatz B, Johansson LF, de Boer EN, et al. Targeted next-generation sequencing can replace Sanger sequencing in clinical diagnostics. *Hum Mutat.* 2013;34:1035–1042.